DynamicBias: Sequence-Aware Calibrated Watermarking for Large Language Models

Anonymous authors
Paper under double-blind review

Abstract

Text watermarking has attracted significant research interest as a way to mitigate LLM-related harms by enabling reliable identification of machine-generated text. In particular, "green" and "red" vocabulary-partition watermarking, which uses a static bias to skew token sampling toward green tokens and away from red, is a promising approach. However, a persistent trade-off remains: stronger watermarks improve detectability but can harm quality, while weaker ones preserve quality but are harder to detect and easier to remove via paraphrasing. A key reason is that the static bias ignores heterogeneous logit distributions across models, domains, and languages, yielding inconsistent performance and hindering practical deployment. Our preliminary investigation shows substantial variability in these distributions and the associated performance disparities, driven by model certainty, measured as the margin between the top logit and the average of a small pool of next-best token logits. Building on this observation, we propose DynamicBias, which calibrates the bias at each step using a sequence-level average of this margin with a single scaling parameter α. Theoretically, we show that DynamicBias admits a unique optimal α and increases expected detectability as the sequence-level margin grows. This calibration yields consistent detectability across models and integrates directly with existing vocabulary-partition watermarks, offering a practical solution for real-world deployment. Extensive experiments across four LLMs and three languages demonstrate improved detection with competitive text quality and stronger robustness to paraphrasing. Our code will be available at `https://github.com/[Anonymous]`.

1 Introduction

The rapid and pervasive adoption of large language models (LLMs) has unlocked powerful generative capabilities across a wide range of applications (Ouyang et al., 2022; OpenAI et al., 2024; Grattafiori et al., 2024; Qwen et al., 2025). It also raises significant concerns about the traceability and authenticity of AI-generated text, including malicious mass generation of misinformation (Zellers et al., 2019; Chen et al., 2023) and academic dishonesty (Stokel-Walker, 2022; Vasilatos et al., 2025), as well as the risk of future models being inadvertently trained on synthetic content (Radford et al., 2022; Shumailov et al., 2024). Watermarking, which embeds distinctive patterns into generated text, has emerged as a critical approach for provenance and copyright protection (Kirchenbauer et al., 2024; Liu et al., 2024b). However, a persistent trade-off hinders practical deployment: stronger watermarks raise detectability but can harm quality, whereas weaker ones preserve quality but reduce detectability and are easier to paraphrase away (Liu et al., 2024b; Giboulot & Furon, 2024; Wu et al., 2024). Therefore, practical deployment demands watermarks that balance quality and detectability.

Decoding-based watermarking embeds identifiable patterns directly in generated text and has been widely studied. A standard approach is KGW, which partitions the vocabulary into "green" and "red" sets via a prefix hash and adds a static positive bias δ to "green" logits during generation to encourage their selection (Kirchenbauer et al., 2024). Despite its simplicity, KGW-based approaches often struggle to balance text quality and detectability (Guo et al., 2024; Ren et al., 2024; Chen et al., 2024; Zhao et al., 2024; Wu & Chandrasekaran, 2024). This instability arises because a static bias ignores heterogeneity in logit distributions across models, domains, and languages. While unbiased watermarking aims to preserve the expected sampling distribution to maintain quality (Kuditipudi et al., 2024; Hu et al., 2024; Wu et al., 2024), current implementations often sacrifice robustness or incur nontrivial computational overhead. Low-entropy watermarking restricts watermarking to uncertain contexts and skips confident tokens (Lu et al., 2024; Liu & Bu, 2024), which helps quality, yet requires the original model at detection time and adds cost. Other works train auxiliary models to improve the trade-off, but these methods are not model-independent and can disrupt end-to-end inference, hindering deployment (Liu et al., 2024a; He et al., 2024; Huo et al., 2024).

Entropy-gated schemes such as SWEET (Lee et al., 2024) gate a static bias δ by entropy, deciding when to apply the watermark. By contrast, dynamic schemes such as MorphMark (Wang et al., 2025) scale the watermark strength (Wouters, 2024; Takezawa et al., 2025) by the cumulative green-list probability mass. However, both operate at the token-level and do not explicitly capture sequence-level variability, making it difficult to balance text quality and detectability across models and domains. Hence, a practical watermark should be adaptable across models and domains. We address this by calibrating the bias with a sequence-aware signal computed from the logits.

In this paper, we first conduct a preliminary study and find substantial variability in next-token logit distributions across models and domains, with corresponding variability in detectability. These differences reflect model certainty, measured as the gap between the top logit and the mean of the second to fifth largest logits. To address this limitation, we propose DynamicBias, a controller designed to work across models, going beyond token-level heuristics and high-entropy-only targeting. At each step, it measures this gap, maintains a sequence-level average, and calibrates the bias with a single scaling parameter α. By aggregating certainty at the sequence level, DynamicBias avoids the under-marking that arises when watermarking is applied only in uncertain regions, thereby preserving quality while improving detectability. Under standard smoothness assumptions, calibrating the bias by the sequence-level margin increases the expected detection statistic in the small-bias regime. DynamicBias integrates directly with vocabulary-partition watermarks.

We conduct experiments and perform an in-depth analysis to demonstrate our proposed method. We use instruction-tuned LLMs from two families: Llama (Grattafiori et al., 2024) and Qwen (Qwen et al., 2025; Yang et al., 2025). We evaluate open-ended generation on C4 (Dodge et al., 2021) and mC4 (Xue et al., 2021), and arithmetic reasoning on GSM8K (Cobbe et al., 2021) and MGSM (Shi et al., 2022) in English, Japanese, and Korean. Experimental results show that integrating DynamicBias into KGW-based methods achieves a better balance between text quality and detectability. Furthermore, DynamicBias remains robust to various paraphrasing attacks, maintaining higher detectability.

Our contributions are summarized as follows: (1) We present preliminary empirical evidence that logit distributions vary substantially across models, domains, and languages, and that this heterogeneity leads to performance disparities for static bias watermarking. (2) We introduce DynamicBias, a sequence-aware mechanism that adapts the bias from a sequence-level average of the logit margin during generation, rather than relying on instantaneous, token-level entropy. (3) We expose a single scaling parameter α that controls bias strength, replacing the ambiguity of a static bias and working across different model families and domains. (4) We demonstrate flexible integration of DynamicBias with existing vocabulary-partition watermarks without modifying hashing, partitioning, or detection.

2 PRELIMINARY

The watermarking process for LLMs has two stages: watermark encoding and detection.

Encoding. Given a prompt $\mathbf{x}_{1:n} = \{x_1, \ldots, x_n\}$, an LLM $\mathcal{M}$ generates a continuation $\mathbf{x}_{n+1:m} = \{x_{n+1}, \ldots, x_m\}$. We formalize decoding-based watermarking below, using KGW as a representative example (Kirchenbauer et al., 2024), which proceeds as follows.

(1) Compute a hash of the current prefix (e.g., using the last token index as input): $h_{n+1} = H(\mathbf{x}_{1:n})$.

(2) Using h_{n+1}, deterministically partition the vocabulary $\mathcal{V}$ into disjoint "green" ($\mathcal{V}_g$) and "red" token sets ($\mathcal{V}_r$).

(3) Let $\ell^{n+1} \in \mathbb{R}^{|\mathcal{V}|}$ be the logits for the next token. Add a static bias δ ($\delta > 0$) to green logits:

$$\tilde{\ell}_i^{n+1} \;=\; \ell_i^{n+1} \;+\; \delta\, \mathbf{1}\{\, v_i \in \mathcal{V}_g \,\}. \tag{1}$$

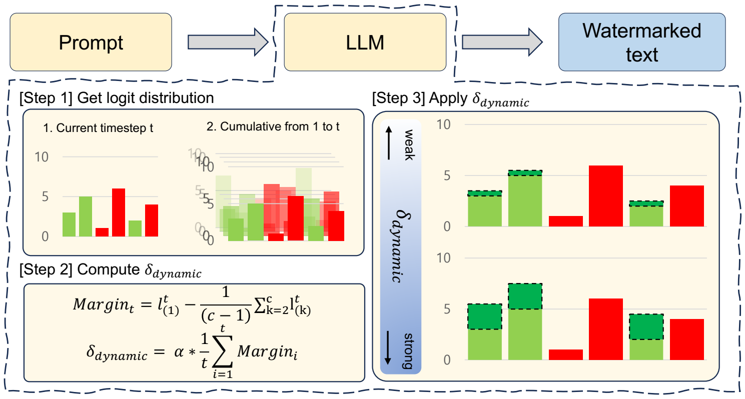
Prompt
LLM
Watermarked text
[Step 1] Get logit distribution
1. Current timestep t
2. Cumulative from 1 to t
10
5
0
[Step 2] Compute $\delta_{dynamic}$
$Margin_t = l^t_{(1)} - \frac{1}{(c-1)} \sum_{k=2}^{c} l^t_{(k)}$
$\delta_{dynamic} = \alpha * \frac{1}{t} \sum_{i=1}^{t} Margin_i$
[Step 3] Apply $\delta_{dynamic}$
weak
$\delta_{dynamic}$
strong
10
5
0

Figure 1: DynamicBias and its sequence-aware calibration.

where i denotes the token index in the vocabulary. Consequently, the bias increases the fraction of "green" tokens in watermarked text relative to typical human text.

Detection. An auditor who knows H and the partitioning rule recomputes steps (1) and (2) on the observed sequence and evaluates a z-score statistic over the realized count of "green" tokens. Let $T = m - n$ be the number of generated tokens and $G = \sum_{t=n+1}^{m} \mathbf{1}\{x_t \in \mathcal{V}_g\}$ with γ denoting the expected fraction of "green" tokens under the null (typically $|\mathcal{V}_g|/|\mathcal{V}|$). The test statistic is

$$z = (G - \gamma T)/\sqrt{T\gamma(1-\gamma)}. \tag{2}$$

The presence of a watermark is determined by comparing the z-score to a pre-defined threshold to test the null hypothesis H_0: *The generated text does not follow the green-list constraint*. If z exceeds the threshold, H_0 is rejected and the watermark is identified.

Motivation and KGW-based framework. Numerous approaches follow the KGW-based (Kirchenbauer et al., 2024) "green" and "red" list design, in which a static bias δ is applied to green-token logits at each step. However, the static bias mechanism remains unchanged (Guo et al., 2024; Ren et al., 2024; Chen et al., 2024; Zhao et al., 2024; Wu & Chandrasekaran, 2024). The effectiveness of this framework hinges on the choice of the scalar hyperparameter δ. A static δ creates a fundamental trade-off between text quality and watermark detectability. A larger δ strengthens the watermark and improves detection power but can noticeably degrade generation quality. Conversely, a smaller δ preserves better fluency yet yields a weak watermark that is difficult to detect reliably. This dilemma is amplified by heterogeneity in next-token logit distributions across models, domains, and languages. Moreover, most existing adaptations operate at the token level, making the bias decision sensitive to local entropy and sampling noise, thereby inducing stepwise fluctuations and unstable detectability (Takezawa et al., 2025; Wouters, 2024; Lee et al., 2024; Wang et al., 2025). A static δ that appears "optimal" in one setting can be suboptimal or even ineffective in another. These observations motivate a sequence-aware approach that is robust across models and domains.

3 METHODOLOGY

We present DynamicBias, a sequence-aware controller that calibrates the bias to the scale of the logits during generation, reducing sensitivity to local noise while retaining a strong signal. It computes a logit-based certainty signal, maintains a sequence-level average, and sets the stepwise bias via a single scaling parameter α.

Figure 1 provides an overview of DynamicBias. It replaces the static δ with a stepwise bias δ_t calibrated by a sequence-level average of the margin. The watermarked logits are

$$\tilde{\ell}_i^t = \ell_i^t + \delta_t \mathbf{1}\{v_i \in \mathcal{V}_g\}, \qquad i = 1, \ldots, |\mathcal{V}|. \tag{3}$$

Compared to Eq. (1), Eq. (3) replaces the static bias δ with a stepwise bias δ_t. No other changes are made to hashing, partitioning, or decoding.

3.1 Certainty Margin

We quantify stepwise certainty using a margin between the top logit and a small pool of next-best logits. Entropy requires a full softmax and can saturate under probability compression, whereas a logit margin avoids softmax and preserves dynamic range. Since watermarking operates in logit space, a logit-based control keeps everything in the same space, reducing scale and/or threshold fragilities and improving stability across models and domains.

Let $\ell^t_{(1)} \geq \ell^t_{(2)} \geq \cdots$ denote the logits sorted in descending order. Define the instantaneous margin

$$m_t = \ell^t_{(1)} - \frac{1}{c-1} \sum_{k=2}^{c} \ell^t_{(k)}. \tag{4}$$

where *c* is a small integer specifying how many of the next-best logits are averaged. This margin is a stable proxy for certainty: it is less sensitive to tail noise than entropy and requires no access to model internals beyond the logits.

3.2 Sequence-Aware Calibration

To avoid reacting to token-level noise, we maintain a sequence-level average of the margin over the generated steps. Let $t \in \{n+1, \ldots, m\}$ and define the number of tokens generated so far as $K_t = t - n$. Define

$$\bar{m}_t = \frac{1}{K_t} \sum_{s=n+1}^{t} m_s, \tag{5}$$

where $\bar{m}_{n+1} = m_{n+1}$. Equivalently, we can update $\bar{m}_t$ recursively, without storing past margins:

$$\bar{m}_t = \bar{m}_{t-1} + \frac{m_t - \bar{m}_{t-1}}{K_t}. \tag{6}$$

We then set the stepwise bias by a single parameter $\alpha > 0$ as $\delta_t = \alpha \bar{m}_t$. When the current top token is red, a sufficient condition for a flip to green at step *t* is $\alpha s_t \geq L_r - L_g$, where s_t is the control signal and L_r and L_g are the logits of the top red and top green candidates, respectively. With $s_t = m_t$, this condition often fails in uncertain regions because m_t shrinks precisely when a flip is needed. Using $s_t = \bar{m}_t$ carries confidence from earlier steps, so $\alpha \bar{m}_t \geq L_r - L_g$ holds more frequently and selections are more stable across models.

3.3 Direction of Adaptation and Detection

When the model is confident (large $\bar{m}_t$), a given green-list bias induces a smaller distortion of relative probabilities. Our calibration therefore increases δ_t with $\bar{m}_t$, improving detectability while preserving quality. When the model is uncertain (small $\bar{m}_t$), the bias is correspondingly small, thereby avoiding over-biasing and maintaining fluency.

For detection, we use the standard *z*-score test used in KGW, SWEET, and MorphMark (Kirchenbauer et al., 2024; Lee et al., 2024; Wang et al., 2025).

3.4 Theoretical Analysis

Under a fixed KGW partition $(\mathcal{V}_g, \mathcal{V}_r)$ at step *t*, let $p_t(i) \propto e^{\ell^t_i}$ and $p^g_t = \sum_{i \in \mathcal{V}_g} p_t(i)$. For a small green-list bias $\delta_t > 0$, the watermarked logits are $\tilde{\ell}^t_i = \ell^t_i + \delta_t \mathbf{1}\{i \in \mathcal{V}_g\}$.

Lemma 1 (First-order green-mass gain). *For small δ_t, $\Delta p^g_t \approx \beta_t \delta_t, \beta_t = p^g_t(0)\big(1 - p^g_t(0)\big)$, where $p^g_t(0)$ is the green mass at zero bias. (See Appendix A.1 for the proof).*

Lemma 2 (Quadratic local cost). *For smooth quality metrics (e.g., KL, Bhattacharyya), the per-step quality loss admits a local quadratic form QualityLoss$_t \approx \kappa_t \delta_t^2, \kappa_t > 0$, and under a local KL proxy one may take $\kappa_t \simeq \frac{1}{2} \beta_t$. (See Appendix A.2 for the proof).*

Let T be the number of generated tokens and $\gamma = |\mathcal{V}_g|/|\mathcal{V}|$ the null green fraction. Since

$$\mathbb{E}[z] = \frac{1}{\sqrt{T\,\gamma(1-\gamma)}} \sum_t (p^g_t - \gamma), \quad \Longrightarrow \quad \Delta\mathbb{E}[z] \approx \frac{1}{\sqrt{T\,\gamma(1-\gamma)}} \sum_t \Delta p^g_t \propto G(\boldsymbol{\delta}),$$

maximizing the linear surrogate gain $G(\boldsymbol{\delta}) = \sum_t \beta_t \, \delta_t$ under a quadratic cost budget $C(\boldsymbol{\delta}) = \sum_t \kappa_t \, \delta_t^2 \leq B$ approximately increases the expected z-score in the small-bias regime. Here, $B > 0$ denotes a global cost budget that upper-bounds the cumulative quadratic loss $C(\boldsymbol{\delta})$.

Theorem 1 (DynamicBias calibration). *Introduce a positive weight ω to trade off gain and cost. DynamicBias sets $\delta_t = \alpha \, \bar{m}_t$, where $\bar{m}_t$ is the sequence-level average of a logit-margin signal and $\alpha > 0$ is a scalar. Define $S = \sum_t \beta_t \, \bar{m}_t, K = \sum_t \kappa_t \bar{m}_t^2$. Then, $G(\alpha) = \alpha S$ and $C(\alpha) = \alpha^2 K$, and the Lagrangian-style objective:*

$$F_\omega(\alpha) = \omega \, S \, \alpha - K \, \alpha^2$$

is strictly concave in α with the unique maximizer

$$\alpha^* = \frac{\omega S}{2K} \in (0, \infty), \qquad \frac{\partial \alpha^*}{\partial S} = \frac{\omega}{2K} > 0, \qquad \frac{\partial \alpha^*}{\partial K} = -\frac{\omega S}{2K^2} < 0.$$

(See Appendix A.3 for the proof).

As the sequence-level margin contribution S grows (i.e., the model is more confident on average), the optimal scale α^* increases, yielding larger expected detectability for a given cost; if the cost curvature K grows, α^* should decrease.

Relation to MorphMark. MorphMark's Theorem 1 establishes token-level monotonicity of the optimal strength with respect to the green-mass signal in a probability-reweighting scheme (Wang et al., 2025). Our analysis instead targets KGW-style additive logit bias with a sequence-level margin controller. Hence, their token-level theorem does not transfer directly to our parameterization (Takezawa et al., 2025; Wouters, 2024). Empirically, we observe trends consistent with the token-level theory while gaining stability from sequence-level averaging.

4 Experiments

4.1 Experimental Setup

Datasets. We evaluate watermarking methods on both open-ended generation and reasoning tasks across multiple languages. (1) C4 and mC4: We use the C4 dataset as prompts for open-ended continuation. For the Japanese and Korean datasets, we utilize the mC4 dataset, which consists of web-scraped content from Common Crawl (Xue et al., 2021). For both C4 and mC4, we randomly sample 500 instances from each test set by following previous work (Kirchenbauer et al., 2024; Guo et al., 2024; Kuditipudi et al., 2024). (2) GSM8K and MGSM: For arithmetic reasoning, we use the GSM8K benchmark of grade-school math word problems. For the Japanese dataset, we employ the MGSM benchmark (Shi et al., 2022), which contains 250 test instances per language. In the MGSM experiments, we use eight training instances as few-shot examples. For the Korean dataset, due to the absence of an original MGSM dataset, we utilize a translated version of GSM8K.[1]

Evaluation Metrics. For text quality, we follow prior work (Ren et al., 2024; Kirchenbauer et al., 2024; Guo et al., 2024; Chen et al., 2024; Lu et al., 2024) and report perplexity (PPL) on the C4 and mC4 datasets. For assessing mathematical reasoning capability, we measure accuracy based on the correctness of the model's generated solutions. To evaluate detection performance, we utilize the area under the receiver operating characteristic curve (AUC), a standard metric for binary classification. Due to limited space, we report TPR at FPR≤5% (TPR@5) for detectability in Appendix Tables.

Baselines. KGW is a vanilla watermarking method that partitions the LLM vocabulary into "green" and "red" token sets to enable detection of watermarked text (Kirchenbauer et al., 2024). **Unigram** fixes the green set via a fixed hash key within KGW to improve robustness (Zhao et al., 2024). **UPV** (Liu et al., 2024a) proposes a cryptographically secure scheme that enables public verification through an auxiliary detector. We integrate **DynamicBias** into KGW, Unigram, and UPV. We also compare against **SWEET**, which applies watermarking only in high-entropy contexts (Lee et al., 2024), and **MorphMark**, which adaptively scales the bias according to the token-level green probability mass (Wang et al., 2025).

[1] `https://huggingface.co/datasets/ChuGyouk/GSM8K-Ko`

Table 1: Performance averaged over four LLMs for each method. +D indicates DynamicBias is applied. **Bold** denotes improvements when DynamicBias is applied. Un-Water indicates no watermarking.

Method	C4 (PPL ↓ / AUC ↑)								GSM8K (ACC ↑ / AUC ↑)							
	EN		KR		JA		AVG		EN		KR		JA		AVG	
	PPL	AUC	PPL	AUC	PPL	AUC	PPL	AUC	ACC	AUC	ACC	AUC	ACC	AUC	ACC	AUC
Un-Water	4.25	-	3.81	-	4.14	-	4.07	-	56.28	-	9.39	-	8.89	-	24.85	-
KGW	6.52	0.991	6.34	0.960	6.75	0.971	6.79	0.978	53.47	0.848	8.19	0.861	8.28	0.884	23.31	0.864
Unigram	6.45	0.990	5.28	0.967	6.18	0.971	6.14	0.979	52.47	0.814	7.92	0.857	8.02	0.889	22.80	0.853
UPV	6.11	0.992	5.27	0.937	5.66	0.942	5.76	0.958	52.12	0.784	7.85	0.808	7.71	0.834	22.56	0.809
SWEET	6.02	0.989	5.79	0.958	6.18	0.966	6.32	0.975	53.56	0.772	8.47	0.846	8.36	0.863	23.46	0.827
MorphMark	4.40	0.934	4.05	0.880	4.30	0.871	4.25	0.895	57.51	0.663	8.89	0.691	8.85	0.726	25.08	0.693
KGW+D	**5.32**	**0.996**	**5.43**	**0.983**	**6.02**	**0.985**	**5.80**	**0.989**	51.44	**0.966**	8.12	**0.949**	**8.47**	**0.958**	22.68	**0.958**
Unigram+D	**5.23**	**0.993**	**4.97**	**0.980**	**5.75**	**0.978**	**5.50**	**0.986**	51.21	**0.946**	**8.30**	**0.909**	7.77	**0.941**	22.43	**0.932**
UPV+D	**5.23**	**0.995**	**5.04**	**0.961**	**5.48**	**0.960**	**5.35**	**0.967**	47.86	**0.934**	7.58	**0.895**	7.43	**0.915**	20.96	**0.915**

Models and Implementation Details. We evaluate four LLMs from two families: Llama3.2-3B-Instruct (Grattafiori et al., 2024), Qwen2.5-3B-Instruct (Qwen et al., 2025), Qwen3-1.7B, and Qwen3-4B (Yang et al., 2025). To evaluate PPL, we employ the Qwen-2.5-14B instruction-tuned model. Following prior work, we employ greedy decoding (Chen et al., 2024; Guan et al., 2024; Kirchenbauer et al., 2024). For baseline watermarkings, we apply $\gamma = 0.3$ and $\delta = 3.0$ (Chen et al., 2024). We set the minimum generation length to 50 and the maximum to 200. We apply DynamicBias with a stepwise bias $\delta_t = \alpha \bar{m}_t$ with $\alpha = 0.45$. For the certainty margin, we use $c = 5$. We reset $\bar{m}_t$ for every new prompt to avoid cross-sequence contamination. We use MarkLLM, an open-source toolkit for LLM watermarking, and carefully implement all baselines (Pan et al., 2024). Detailed settings are in Appendix A.4.

4.2 Preliminary Investigation

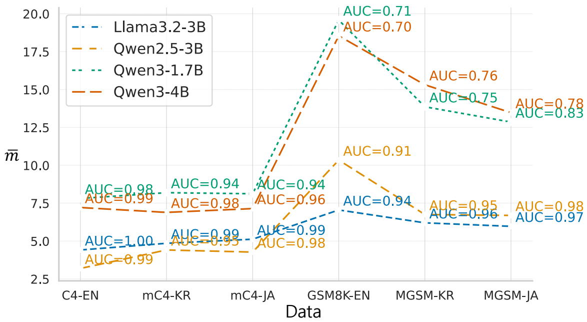

Figure 2: Sequence-averaged logit gap and detectability. The x-axis denotes datasets; the y-axis denotes the top logit minus the mean of ranks 2-5.

We first conducted a preliminary study to quantify the relationship between the next-token logit distribution, on which a static bias δ is applied, and detection performance. Figure 2 shows that settings with small logit gaps achieve very high detectability, whereas settings with large gaps exhibit marked drops in AUC. Using the Unigram watermark, we observed a strong negative correlation between the sequence-averaged logit gap and AUC (Pearson $r = -0.960$). These results indicate that a static bias is not universally optimal: a value tuned for one model or domain can be too weak or too strong in others, yielding inconsistent performance. They support our hypothesis from the introduction that the static bias ignores heterogeneity in logit distributions across models, domains, and languages, and therefore does not generalize reliably. With a static bias δ, small-gap settings often yield higher detectability because the same additive shift moves relatively more mass from the red to the green partition; however, this also risks quality degradation. Conversely, in large-gap settings, the shift causes less relative distortion, tending to preserve quality but weakening the watermark signal and reducing AUC.

4.3 Overall Performance

Table 1 shows results averaged over four LLMs. Per-model results are in Appendix B.1. Incorporating DynamicBias into KGW, Unigram, and UPV consistently improves detectability across all baselines. For C4 and mC4, AUC increases with DynamicBias while perplexity decreases. For GSM8K and MGSM, applying DynamicBias to KGW, Unigram, and UPV yields larger AUC gains, with a slight drop in accuracy. SWEET achieves higher AUC than MorphMark on C4 and mC4 but struggles on GSM8K and MGSM, whereas MorphMark shows weaker detectability overall. While DynamicBias improves detection performance without sacrificing text quality, its gains are smaller in non-English languages. We think this is because of language-specific differences in logit margins. Additional experimental results comparing our method with the method that uses an auxiliary model for learning bias are provided in Appendix B.2.

4.4 Performance on Robustness

Because paraphrasing can diminish watermark signals, we evaluate three paraphrasing attacks to assess robustness. First, WordDel randomly deletes 50% of words from the text. Second, WordSub randomly replaces 50% of words with synonyms from WordNet. Third, Dipper rewrites the text with a specialized paraphrasing model. Table 2 shows the results using Qwen3-4B. As shown, DynamicBias improves detectability for KGW, Unigram, and UPV under all attacks. These results indicate that DynamicBias is more robust and therefore more practical and reliable.

Table 2: AUC under attacks on C4 and GSM8K.

Method	C4 (AUC ↑)				GSM8K (AUC ↑)			
	Original	WordDel	WordSub	Dipper	Original	WordDel	WordSub	Dipper
KGW	0.997	0.934	0.825	0.787	0.824	0.669	0.581	0.739
Unigram	0.995	0.983	0.921	0.914	0.698	0.607	0.583	0.595
UPV	0.991	0.932	0.852	0.804	0.668	0.575	0.551	0.417
KGW+D	**0.998**	**0.939**	**0.841**	**0.794**	**0.974**	**0.793**	**0.681**	**0.752**
Unigram+D	**0.997**	**0.988**	**0.942**	**0.918**	**0.916**	**0.804**	**0.766**	**0.655**
UPV+D	**0.995**	**0.959**	**0.855**	**0.808**	**0.900**	**0.689**	**0.639**	**0.445**

4.5 Performance on Text Quality and in Low-Entropy Scenarios

To evaluate text quality beyond PPL and in low-entropy settings, we conduct experiments on CNN/DM for document summarization (Hermann et al., 2015) and HumanEval for code generation (Chen et al., 2021). For summarization, we use ROUGE-L (R-L) (Lin, 2004) and BERTScore (BS) (Zhang et al., 2020). For code generation, we use Pass@1. We keep the same parameters as in the main study. Table 3 shows the results using Qwen3-4B. DynamicBias substantially improves detectability with acceptable drops in R-L, BS, and Pass@1. These small decreases reflect the quality and detectability trade-off, while AUC increases markedly. Details on the datasets and settings are in Appendix C.

Table 3: CNN/DM summarization and HumanEval code generation.

Method	CNN/DM			HumanEval	
	R-L↑	BS↑	AUC↑	Pass@1↑	AUC↑
KGW	28.33	63.57	0.908	0.3598	0.602
Unigram	29.56	64.87	0.896	0.3841	0.558
UPV	29.47	65.02	0.901	0.3354	0.601
SWEET	29.21	64.41	0.752	0.3841	0.504
MorphMark	29.69	64.72	0.714	0.3902	0.525
KGW+D	27.00	63.06	**0.996**	0.3049	**0.818**
Unigram+D	29.43	64.63	**0.985**	0.3537	**0.675**
UPV+D	28.35	64.44	**0.985**	0.3232	**0.788**

4.6 Bin-Wise Analysis for Detection Performance

Table 4 shows the results for the bin-wise analysis on the C4 and mC4 datasets. By using Qwen3-4B, we group generations by sequence length and compute detection performance per bin, confirming that DynamicBias maintains strong detection even for short outputs.

Table 4: AUC and TPR@5 across token-range segments.

Data	Method	0–25		25–50		50–75		75–100	
		AUC	TPR@5	AUC	TPR@5	AUC	TPR@5	AUC	TPR@5
C4-EN	KGW	0.93	0.71	0.98	0.89	0.99	0.94	0.99	0.98
	KGW+D	**0.95**	**0.79**	**0.98**	**0.92**	**0.99**	**0.97**	**1.0**	**0.99**
mC4-KR	KGW	0.89	0.59	0.94	0.75	0.96	0.89	0.97	0.91
	KGW+D	**0.93**	**0.68**	**0.96**	**0.82**	**0.98**	**0.91**	**0.99**	**0.95**
mC4-JA	KGW	0.85	0.50	0.92	0.78	0.95	0.84	0.96	0.89
	KGW+D	**0.89**	**0.59**	**0.95**	**0.84**	**0.97**	**0.90**	**1.0**	**1.0**

4.7 Ablation Study for α and γ

In this section, we ablate the hyper-parameters of DynamicBias, including α for scaling the bias and γ for the green vocabulary proportion. A larger α applies a stronger bias, whereas a smaller α applies a weaker bias. A larger γ indicates a higher proportion of green tokens, whereas a smaller γ denotes a lower green proportion. Figure 3 (a) shows the results of varying α while keeping other settings fixed. As α increases, the z-score on C4 grows almost linearly and PPL increases slowly. On GSM8K, the z-score also rises with α, while accuracy begins to decrease once α becomes large. Quantitatively, the z-score scales nearly linearly with α (C4: R^2=0.9992, GSM8K: R^2=0.9747),

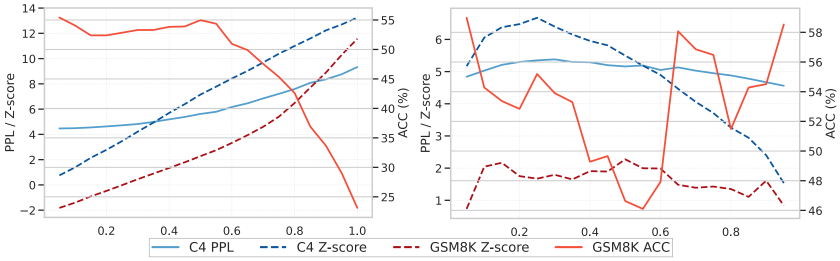

Figure 3: Parameter ablation study of DynamicBias using Qwen3-4B. DynamicBias is applied to KGW. In (a), we ablate α. In (b), we ablate γ. Scores are averaged within each dataset.

whereas quality exhibits mild quadratic curvature (PPL: R^2=0.9991, ACC: R^2=0.9574), supporting the small-bias linear-gain and low-curvature cost assumptions used in our calibration analysis.

Figure 3 (b) shows the results of varying γ. On C4, the z-score is higher at small γ and then drops as γ grows, while PPL remains relatively stable. On GSM8K, which contains many numbers and requires math reasoning, very low γ (e.g., 0.1) makes the watermark less responsive and yields a very low z-score. As γ increases, more tokens are steered into the green set, detectability improves, and the z-score rises, while accuracy drops slightly due to increased watermark responsiveness. Once γ exceeds about 0.6, many numeric tokens fall into the green set, reducing distortion on key tokens; accuracy rises again, but AUC decreases as the signal becomes diluted.

Therefore, α smoothly controls watermark strength and should be set to a moderate value, whereas γ should remain small to avoid diluting the signal.

4.8 Ablation Study for c and Sequence-Aware Calibration

Table 5: Effect of the pool size c in the margin definition.

c	C4		GSM8K		HumanEval	
	PPL↓	AUC↑	ACC↑	AUC↑	Pass@1↑	AUC↑
2	**5.10**	0.983	23.70	0.883	**0.317**	0.738
5	5.79	0.994	**25.09**	0.940	0.305	0.818
10	6.52	**0.996**	24.79	**0.975**	0.287	**0.853**

We vary the pool size c in the margin definition by using Top-2 ($c = 2$), Top-2-5 ($c = 5$), and Top-2-10 ($c = 10$). Table 5 shows the results using Qwen3-4B, averaged over English, Japanese, and Korean. Per-language results are in Appendix B.3. On C4 and HumanEval, AUC increases as c grows, while PPL and Pass@1 degrade moderately. On GSM8K, AUC also increases with c, and accuracy is largely stable, with a mild peak around $c = 5$ on average. This trend is expected: as c grows, the next-best pool includes lower-ranked logits, the averaged competitor score declines, the margin becomes larger, and the calibrated bias increases accordingly. Thus, averaging over a larger set of next-best logits reduces variance in the certainty estimate and yields a steadier bias schedule, improving detectability. However, very large c values slightly inflate PPL and can nudge accuracy down in some languages.

Table 6: Performance of sequence-aware calibration and token-level DynamicBias.

Scope	C4		GSM8K	
	PPL↓	AUC↑	ACC↑	AUC↑
Morphmark ($k_{linear} = 1.55$)	4.57	0.886	26.21	0.605
Morphmark ($k_{linear} = 9.0$)	5.42	0.985	26.05	0.747
Token	**4.75**	0.894	**26.61**	0.716
Sequence	5.79	**0.994**	25.09	**0.940**

Table 6 shows the effect of sequence-aware calibration versus a token-level variant using Qwen3-4B, averaged over English, Japanese, and Korean. The token-level variant skips sequence-aware calibration (Sec. 3.2) and uses $\delta_t = \alpha m_t$. We also include results obtained by increasing the MorphMark detection parameter, which is k_{linear}, calibrated on the C4 dataset. MorphMark shows limited gains in detection performance and struggles on GSM8K. Sequence-aware calibration delivers higher AUC at a small cost in PPL, with minimal accuracy change. These results are consistent with the intuition that sequence-level averaging increases the effective bias when it matters, making $\alpha \bar{m}_t \geq L_r - L_g$ more often satisfied and yielding green selections. Per-language results and detailed tuning results are in Appendix B.4.

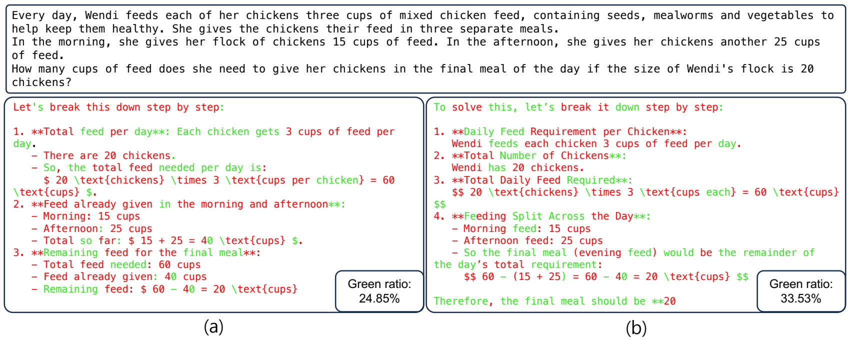

```
Every day, Wendi feeds each of her chickens three cups of mixed chicken feed, containing seeds, mealworms and vegetables to
help keep them healthy. She gives the chickens their feed in three separate meals.
In the morning, she gives her flock of chickens 15 cups of feed. In the afternoon, she gives her chickens another 25 cups
of feed.
How many cups of feed does she need to give her chickens in the final meal of the day if the size of Wendi's flock is 20
chickens?
```

```
Let's break this down step by step:

1. **Total feed per day**: Each chicken gets 3 cups of feed per
day.
   - There are 20 chickens.
   - So, the total feed needed per day is:
     $ 20 \text{chickens} \times 3 \text{cups per chicken} = 60
\text{cups} $.
2. **Feed already given in the morning and afternoon**:
   - Morning: 15 cups
   - Afternoon: 25 cups
   - Total so far: $ 15 + 25 = 40 \text{cups} $.
3. **Remaining feed for the final meal**:
   - Total feed needed: 60 cups
   - Feed already given: 40 cups
   - Remaining feed: $ 60 - 40 = 20 \text{cups}
```

Green ratio: 24.85%

(a)

```
To solve this, let’s break it down step by step:

1. **Daily Feed Requirement per Chicken**:
   Wendi feeds each chicken 3 cups of feed per day.
2. **Total Number of Chickens**:
   Wendi has 20 chickens.
3. **Total Daily Feed Required**:
   $$ 20 \text{chickens} \times 3 \text{cups each} = 60 \text{cups}
$$
4. **Feeding Split Across the Day**:
   - Morning feed: 15 cups
   - Afternoon feed: 25 cups
   - So the final meal (evening feed) would be the remainder of
the day’s total requirement:
     $$ 60 - (15 + 25) = 60 - 40 = 20 \text{cups} $$

Therefore, the final meal should be **20
```

Green ratio: 33.53%

(b)

Figure 4: Case study on GSM8K. (a) shows KGW and (b) shows KGW+D. The black text represents the input prompt. green and red highlights mark tokens in the green and red lists, respectively.

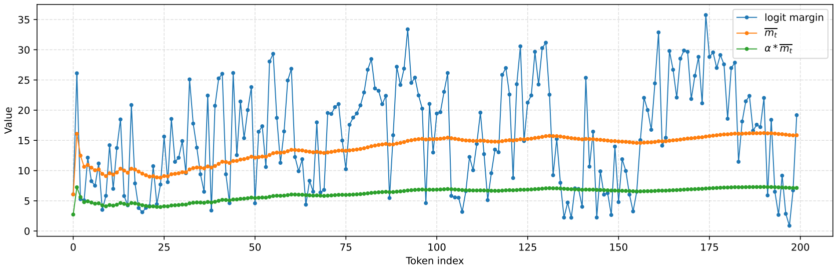

Figure 5: Visualization of the the Top-2-5 logit margin ($c = 5$), $\bar{m}_t$, and its scaled version $\alpha\bar{m}_t$ for DynamicBias in (b) of Figure 4. The x-axis indicates the token index and the y-axis shows their values.

4.9 Runtime Comparison

In addition to text quality and detection performance, we compare the runtime overhead of different watermarking methods. We measure both generation and detection time using NVIDIA A6000 GPU. We sampled 100 instances from the C4 dataset by generating 200 tokens for each instance. Table 7 shows the results. DynamicBias does not significantly increase generation time compared to the baseline methods. At detection time, it incurs almost no additional overhead because it does not require computing token entropies or querying the model.

Table 7: Latency comparison across watermarking methods and models.

Model	Method	Gen. Time (token/ms)	Gen. Time (data/s)	Detect. Time (data/ms)
Llama 3.2 -3B	KGW	**26.28**	**5.25**	**24.9**
	KGW + D	26.41	5.28	25.0
	UPV	28.61	5.71	38.5
	UPV + D	28.74	5.74	38.9
	SWEET	26.37	5.27	133.6
	Morphmark	26.64	5.28	26.8
Qwen 3 -4B	KGW	**34.93**	**6.97**	**26.2**
	KGW + D	35.17	7.03	26.3
	UPV	37.92	7.57	44.1
	UPV + D	38.03	7.61	44.6
	SWEET	35.18	7.01	163.4
	Morphmark	35.54	7.06	28.1

4.10 Case Study

We present a case study using Qwen3-4B between KGW and KGW+DynamicBias (KGW+D) on a GSM8K example, using identical parameter settings. Figure 4 shows the results. We observe that KGW+D generates more green tokens than KGW, resulting in higher detectability and greater robustness to paraphrasing attacks. Appendix B.5 includes the average number of green tokens across datasets. Figure 5 shows the evolution of δ_t over token steps. Although the second token spikes, the averaged and scaled margins remain stable.

4.11 Decoding Strategy

We test whether DynamicBias remains effective under different sampling parameters at the decoding stage. We consider top-p sampling at 0.95 with temperature 0.7. Table 8 shows the results averaged over four LLMs. DynamicBias achieves a superior balance between text quality and detectability. Per-model results are in Appendix B.6.

Table 8: Performance averaged over four LLMs with top-p sampling.

Method	C4 (PPL ↓ / AUC ↑)								GSM8K (ACC ↑ / AUC ↑)							
	EN		KR		JA		AVG		EN		KR		JA		AVG	
	PPL	AUC	PPL	AUC	PPL	AUC	PPL	AUC	ACC	AUC	ACC	AUC	ACC	AUC	ACC	AUC
Un-Water	4.58	-	4.31	-	4.79	-	4.56	-	56.43	-	9.34	-	8.78	-	24.85	-
KGW	7.23	0.992	7.89	0.964	8.23	0.975	7.78	0.977	52.60	0.849	8.38	0.863	8.13	0.888	23.04	0.867
Unigram	7.17	0.990	6.40	0.972	7.62	0.973	7.06	0.978	52.12	0.813	7.62	0.858	7.62	0.897	22.45	0.856
UPV	6.67	0.992	6.02	0.941	6.57	0.949	6.42	0.961	51.48	0.785	7.83	0.813	7.66	0.841	22.32	0.813
SWEET	6.59	0.990	7.27	0.959	7.55	0.968	7.13	0.972	53.47	0.769	8.61	0.842	8.17	0.863	23.42	0.825
MorphMark	4.70	0.933	4.59	0.882	4.89	0.877	4.73	0.897	56.94	0.665	8.68	0.686	8.83	0.718	24.82	0.690
KGW+D	**5.68**	**0.997**	**6.48**	**0.985**	**7.03**	**0.987**	**6.40**	**0.990**	51.33	**0.966**	8.25	**0.952**	**8.23**	**0.962**	22.60	**0.960**
Unigram+D	**5.65**	**0.992**	**6.17**	**0.983**	**7.03**	**0.979**	**6.28**	**0.985**	50.59	**0.949**	**8.24**	**0.911**	**7.70**	**0.946**	22.17	**0.935**
UPV+D	**5.67**	**0.995**	**5.48**	**0.959**	**6.29**	**0.959**	**5.93**	**0.971**	47.99	**0.912**	7.49	**0.873**	**7.68**	**0.900**	21.05	**0.895**

5 RELATED WORK

Early work framed AI-generated text detection as binary classification over finalized text (Jawahar et al., 2020; Mitchell et al., 2023), but performance degrades as LLM fluency and paraphrasing improve. Decoding-based watermarking instead perturbs logits during generation to embed a statistical signature without retraining.

KGW partitions the vocabulary into “green” and “red” sets via a prefix hash and adds a static bias to “green” logits (Kirchenbauer et al., 2024). Variants strengthen robustness by fixing the green set with a hash key (Zhao et al., 2024), imposing mutual-exclusivity constraints (Chen et al., 2024), and enabling public verification with an auxiliary detector (Liu et al., 2024a). Despite progress, static bias schemes face a trade-off between text quality and detectability under model, domain, and language shifts (Guo et al., 2024; Ren et al., 2024; Wu & Chandrasekaran, 2024). Unbiased watermarking preserves the expected sampling distribution to protect quality (Kuditipudi et al., 2024; Hu et al., 2024; Wu et al., 2024), but current implementations often reduce robustness or add nontrivial overhead. While gating a static bias by entropy to target high-entropy contexts (Lee et al., 2024) and scaling bias strength using the token-level cumulative probability mass on the “green” list (Wang et al., 2025) have been studied, these approaches do not explicitly consider sequence-level variability, limiting stability across settings. Paraphrasing and light edits can weaken watermark signals. Previous works show AUC drops for static bias methods under deletion, substitution, and model-based rewrites (Guo et al., 2024; Ren et al., 2024; Wu & Chandrasekaran, 2024). Approaches that rely on auxiliary detectors or model access can improve robustness but reduce the simplicity of model-independent deployment (Liu et al., 2024a).

DynamicBias is a sequence-aware calibration approach for vocabulary-partition watermarks: it replaces the static bias with one calibrated by a sequence-level margin, leaving hashing, partitioning, and detection unchanged. Unlike unbiased methods, it retains the standard detector; unlike entropy-gated schemes, it does not skip low-entropy tokens; unlike token-level scaling, it aggregates certainty over the sequence to reduce stepwise variance. Our theoretical and empirical results show that this improves detectability while maintaining competitive quality and increases paraphrase robustness.

6 CONCLUSION

We introduced DynamicBias, a sequence-aware controller that replaces the static bias with one calibrated to the scale of next-token logits. The method computes a margin between the top logit and a small pool of next-best logits, averages it over the sequence, and sets a stepwise bias via a single scaling parameter α. Across four LLMs and three languages, DynamicBias improves detectability while maintaining text quality, and it remains effective under paraphrasing attacks. Furthermore, DynamicBias works across different models and domains and integrates easily with vocabulary-partition watermarks. In the future, we will extend DynamicBias beyond vocabulary partitioning and explore learning α.

7 Ethics Statement

All datasets used in this study are publicly available resources from the research community. We did not create or collect any new sensitive content. Beyond introducing a new watermarking framework, our work also provides theoretical analysis to help the community better understand vocabulary-partition watermarking. We believe this contributes positively to the development of safer and more robust LLMs.

8 Reproducibility Statement

All four models used in our experiments (`Llama3.2-3B-Instruct`, `Qwen2.5-3B-Instruct`, `Qwen3-1.7B`, and `Qwen3-4B`) are open-source and publicly available. To facilitate replication, we will release our source code and results, with detailed explanations, to fully reproduce our results. We note that our methods are applicable to models that provide access to top-k log probabilities.

References

Liang Chen, Yang Deng, Yatao Bian, Zeyu Qin, Bingzhe Wu, Tat-Seng Chua, and Kam-Fai Wong. Beyond factuality: A comprehensive evaluation of large language models as knowledge generators. In Houda Bouamor, Juan Pino, and Kalika Bali (eds.), *Proceedings of the 2023 Conference on Empirical Methods in Natural Language Processing*, pp. 6325–6341, Singapore, December 2023. Association for Computational Linguistics. doi: 10.18653/v1/2023.emnlp-main.390. URL https://aclanthology.org/2023.emnlp-main.390/.

Liang Chen, Yatao Bian, Yang Deng, Deng Cai, Shuaiyi Li, Peilin Zhao, and Kam-Fai Wong. WatME: Towards lossless watermarking through lexical redundancy. In Lun-Wei Ku, Andre Martins, and Vivek Srikumar (eds.), *Proceedings of the 62nd Annual Meeting of the Association for Computational Linguistics (Volume 1: Long Papers)*, pp. 9166–9180, Bangkok, Thailand, August 2024. Association for Computational Linguistics. doi: 10.18653/v1/2024.acl-long.496. URL https://aclanthology.org/2024.acl-long.496/.

Mark Chen, Jerry Tworek, Heewoo Jun, Qiming Yuan, Henrique Ponde de Oliveira Pinto, Jared Kaplan, Harri Edwards, Yuri Burda, Nicholas Joseph, Greg Brockman, Alex Ray, Raul Puri, Gretchen Krueger, Michael Petrov, Heidy Khlaaf, Girish Sastry, Pamela Mishkin, Brooke Chan, Scott Gray, Nick Ryder, Mikhail Pavlov, Alethea Power, Lukasz Kaiser, Mohammad Bavarian, Clemens Winter, Philippe Tillet, Felipe Petroski Such, Dave Cummings, Matthias Plappert, Fotios Chantzis, Elizabeth Barnes, Ariel Herbert-Voss, William Hebgen Guss, Alex Nichol, Alex Paino, Nikolas Tezak, Jie Tang, Igor Babuschkin, Suchir Balaji, Shantanu Jain, William Saunders, Christopher Hesse, Andrew N. Carr, Jan Leike, Josh Achiam, Vedant Misra, Evan Morikawa, Alec Radford, Matthew Knight, Miles Brundage, Mira Murati, Katie Mayer, Peter Welinder, Bob McGrew, Dario Amodei, Sam McCandlish, Ilya Sutskever, and Wojciech Zaremba. Evaluating large language models trained on code, 2021.

Karl Cobbe, Vineet Kosaraju, Mohammad Bavarian, Mark Chen, Heewoo Jun, Lukasz Kaiser, Matthias Plappert, Jerry Tworek, Jacob Hilton, Reiichiro Nakano, Christopher Hesse, and John Schulman. Training verifiers to solve math word problems, 2021. URL https://arxiv.org/abs/2110.14168.

Jesse Dodge, Maarten Sap, Ana Marasović, William Agnew, Gabriel Ilharco, Dirk Groeneveld, Margaret Mitchell, and Matt Gardner. Documenting large webtext corpora: A case study on the colossal clean crawled corpus. In Marie-Francine Moens, Xuanjing Huang, Lucia Specia, and Scott Wen-tau Yih (eds.), *Proceedings of the 2021 Conference on Empirical Methods in Natural Language Processing*, pp. 1286–1305, Online and Punta Cana, Dominican Republic, November 2021. Association for Computational Linguistics. doi: 10.18653/v1/2021.emnlp-main.98. URL https://aclanthology.org/2021.emnlp-main.98/.

Eva Giboulot and Teddy Furon. Watermax: breaking the LLM watermark detectability-robustness-quality trade-off. In *The Thirty-eighth Annual Conference on Neural Information Processing Systems*, 2024. URL https://openreview.net/forum?id=HjeKHxK2VH.

Aaron Grattafiori, Abhimanyu Dubey, Abhinav Jauhri, Abhinav Pandey, Abhishek Kadian, Ahmad Al-Dahle, Aiesha Letman, Akhil Mathur, Alan Schelten, Alex Vaughan, Amy Yang, Angela Fan, Anirudh Goyal, Anthony Hartshorn, Aobo Yang, Archi Mitra, Archie Sravankumar, Artem Korenev, Arthur Hinsvark, Arun Rao, Aston Zhang, Aurelien Rodriguez, Austen Gregerson, Ava Spataru, Baptiste Roziere, Bethany Biron, Binh Tang, Bobbie Chern, Charlotte Caucheteux, Chaya Nayak, Chloe Bi, Chris Marra, Chris McConnell, Christian Keller, Christophe Touret, Chunyang Wu, Corinne Wong, Cristian Canton Ferrer, Cyrus Nikolaidis, Damien Allonsius, Daniel Song, Danielle Pintz, Danny Livshits, Danny Wyatt, David Esiobu, Dhruv Choudhary, Dhruv Mahajan, Diego Garcia-Olano, Diego Perino, Dieuwke Hupkes, Egor Lakomkin, Ehab AlBadawy, Elina Lobanova, Emily Dinan, Eric Michael Smith, Filip Radenovic, Francisco Guzmán, Frank Zhang, Gabriel Synnaeve, Gabrielle Lee, Georgia Lewis Anderson, Govind Thattai, Graeme Nail, Gregoire Mialon, Guan Pang, Guillem Cucurell, Hailey Nguyen, Hannah Korevaar, Hu Xu, Hugo Touvron, Iliyan Zarov, Imanol Arrieta Ibarra, Isabel Kloumann, Ishan Misra, Ivan Evtimov, Jack Zhang, Jade Copet, Jaewon Lee, Jan Geffert, Jana Vranes, Jason Park, Jay Mahadeokar, Jeet Shah, Jelmer van der Linde, Jennifer Billock, Jenny Hong, Jenya Lee, Jeremy Fu, Jianfeng Chi, Jianyu Huang, Jiawen Liu, Jie Wang, Jiecao Yu, Joanna Bitton, Joe Spisak, Jongsoo Park, Joseph Rocca, Joshua Johnstun, Joshua Saxe, Junteng Jia, Kalyan Vasuden Alwala, Karthik Prasad, Kartikeya Upasani, Kate Plawiak, Ke Li, Kenneth Heafield, Kevin Stone, Khalid El-Arini, Krithika Iyer, Kshitiz Malik, Kuenley Chiu, Kunal Bhalla, Kushal Lakhotia, Lauren Rantala-Yeary, Laurens van der Maaten, Lawrence Chen, Liang Tan, Liz Jenkins, Louis Martin, Lovish Madaan, Lubo Malo, Lukas Blecher, Lukas Landzaat, Luke de Oliveira, Madeline Muzzi, Mahesh Pasupuleti, Mannat Singh, Manohar Paluri, Marcin Kardas, Maria Tsimpoukelli, Mathew Oldham, Mathieu Rita, Maya Pavlova, Melanie Kambadur, Mike Lewis, Min Si, Mitesh Kumar Singh, Mona Hassan, Naman Goyal, Narjes Torabi, Nikolay Bashlykov, Nikolay Bogoychev, Niladri Chatterji, Ning Zhang, Olivier Duchenne, Onur Çelebi, Patrick Alrassy, Pengchuan Zhang, Pengwei Li, Petar Vasic, Peter Weng, Prajjwal Bhargava, Pratik Dubal, Praveen Krishnan, Punit Singh Koura, Puxin Xu, Qing He, Qingxiao Dong, Ragavan Srinivasan, Raj Ganapathy, Ramon Calderer, Ricardo Silveira Cabral, Robert Stojnic, Roberta Raileanu, Rohan Maheswari, Rohit Girdhar, Rohit Patel, Romain Sauvestre, Ronnie Polidoro, Roshan Sumbaly, Ross Taylor, Ruan Silva, Rui Hou, Rui Wang, Saghar Hosseini, Sahana Chennabasappa, Sanjay Singh, Sean Bell, Seohyun Sonia Kim, Sergey Edunov, Shaoliang Nie, Sharan Narang, Sharath Raparthy, Sheng Shen, Shengye Wan, Shruti Bhosale, Shun Zhang, Simon Vandenhende, Soumya Batra, Spencer Whitman, Sten Sootla, Stephane Collot, Suchin Gururangan, Sydney Borodinsky, Tamar Herman, Tara Fowler, Tarek Sheasha, Thomas Georgiou, Thomas Scialom, Tobias Speckbacher, Todor Mihaylov, Tong Xiao, Ujjwal Karn, Vedanuj Goswami, Vibhor Gupta, Vignesh Ramanathan, Viktor Kerkez, Vincent Gonguet, Virginie Do, Vish Vogeti, Vítor Albiero, Vladan Petrovic, Weiwei Chu, Wenhan Xiong, Wenyin Fu, Whitney Meers, Xavier Martinet, Xiaodong Wang, Xiaofang Wang, Xiaoqing Ellen Tan, Xide Xia, Xinfeng Xie, Xuchao Jia, Xuewei Wang, Yaelle Goldschlag, Yashesh Gaur, Yasmine Babaei, Yi Wen, Yiwen Song, Yuchen Zhang, Yue Li, Yuning Mao, Zacharie Delpierre Coudert, Zheng Yan, Zhengxing Chen, Zoe Papakipos, Aaditya Singh, Aayushi Srivastava, Abha Jain, Adam Kelsey, Adam Shajnfeld, Adithya Gangidi, Adolfo Victoria, Ahuva Goldstand, Ajay Menon, Ajay Sharma, Alex Boesenberg, Alexei Baevski, Allie Feinstein, Amanda Kallet, Amit Sangani, Amos Teo, Anam Yunus, Andrei Lupu, Andres Alvarado, Andrew Caples, Andrew Gu, Andrew Ho, Andrew Poulton, Andrew Ryan, Ankit Ramchandani, Annie Dong, Annie Franco, Anuj Goyal, Aparajita Saraf, Arkabandhu Chowdhury, Ashley Gabriel, Ashwin Bharambe, Assaf Eisenman, Azadeh Yazdan, Beau James, Ben Maurer, Benjamin Leonhardi, Bernie Huang, Beth Loyd, Beto De Paola, Bhargavi Paranjape, Bing Liu, Bo Wu, Boyu Ni, Braden Hancock, Bram Wasti, Brandon Spence, Brani Stojkovic, Brian Gamido, Britt Montalvo, Carl Parker, Carly Burton, Catalina Mejia, Ce Liu, Changhan Wang, Changkyu Kim, Chao Zhou, Chester Hu, Ching-Hsiang Chu, Chris Cai, Chris Tindal, Christoph Feichtenhofer, Cynthia Gao, Damon Civin, Dana Beaty, Daniel Kreymer, Daniel Li, David Adkins, David Xu, Davide Testuggine, Delia David, Devi Parikh, Diana Liskovich, Didem Foss, Dingkang Wang, Duc Le, Dustin Holland, Edward Dowling, Eissa Jamil, Elaine Montgomery, Eleonora Presani, Emily Hahn, Emily Wood, Eric-Tuan Le, Erik Brinkman, Esteban Arcaute, Evan Dunbar, Evan Smothers, Fei Sun, Felix Kreuk, Feng Tian, Filippos Kokkinos, Firat Ozgenel, Francesco Caggioni, Frank Kanayet, Frank Seide, Gabriela Medina Florez, Gabriella Schwarz, Gada Badeer, Georgia Swee, Gil Halpern, Grant Herman, Grigory Sizov, Guangyi, Zhang, Guna Lakshminarayanan, Hakan Inan, Hamid Shojanazeri, Han Zou, Hannah Wang, Hanwen Zha, Haroun Habeeb, Harrison Rudolph, Helen Suk, Henry Aspegren, Hunter Goldman, Hongyuan Zhan, Ibrahim Damlaj, Igor Molybog, Igor Tufanov, Ilias Leontiadis, Irina-Elena Veliche, Itai Gat, Jake Weissman, James Geboski, James Kohli, Janice Lam, Japhet Asher, Jean-Baptiste Gaya, Jeff Marcus, Jeff Tang, Jennifer Chan, Jenny Zhen, Jeremy Reizenstein, Jeremy Teboul, Jessica Zhong, Jian Jin, Jingyi Yang, Joe Cummings, Jon Carvill, Jon Shepard, Jonathan McPhie, Jonathan Torres, Josh Ginsburg, Junjie Wang, Kai Wu, Kam Hou U, Karan Saxena, Kartikay Khandelwal, Katayoun Zand, Kathy Matosich, Kaushik Veeraraghavan, Kelly Michelena, Keqian Li, Kiran Jagadeesh, Kun Huang, Kunal Chawla, Kyle Huang, Lailin Chen, Lakshya Garg, Lavender A, Leandro Silva, Lee Bell, Lei Zhang, Liangpeng Guo, Licheng Yu, Liron Moshkovich, Luca Wehrstedt, Madian Khabsa, Manav Avalani, Manish Bhatt, Martynas Mankus, Matan Hasson, Matthew Lennie, Matthias Reso, Maxim Groshev, Maxim Naumov, Maya Lathi, Meghan Keneally, Miao Liu, Michael L. Seltzer, Michal Valko, Michelle Restrepo, Mihir Patel, Mik Vyatskov, Mikayel Samvelyan, Mike Clark, Mike Macey, Mike Wang, Miquel Jubert Hermoso, Mo Metanat, Mohammad Rastegari, Munish Bansal, Nandhini Santhanam, Natascha Parks, Natasha White, Navyata Bawa, Nayan Singhal, Nick Egebo, Nicolas Usunier, Nikhil Mehta, Nikolay Pavlovich Laptev, Ning Dong, Norman Cheng, Oleg Chernoguz, Olivia Hart, Omkar Salpekar, Ozlem Kalinli, Parkin Kent, Parth Parekh, Paul Saab, Pavan Balaji, Pedro Rittner, Philip Bontrager, Pierre Roux, Piotr Dollar, Polina Zvyagina, Prashant Ratanchandani, Pritish Yuvraj, Qian Liang, Rachad Alao, Rachel Rodriguez, Rafi Ayub, Raghotham Murthy, Raghu Nayani, Rahul Mitra, Rangaprabhu Parthasarathy, Raymond Li, Rebekkah Hogan, Robin Battey, Rocky Wang, Russ Howes, Ruty Rinott, Sachin Mehta, Sachin Siby, Sai Jayesh Bondu, Samyak Datta, Sara Chugh, Sara Hunt, Sargun Dhillon, Sasha Sidorov, Satadru Pan, Saurabh Mahajan, Saurabh Verma, Seiji Yamamoto, Sharadh Ramaswamy, Shaun Lindsay, Shaun Lindsay, Sheng Feng, Shenghao Lin, Shengxin Cindy Zha, Shishir Patil, Shiva Shankar, Shuqiang Zhang, Shuqiang Zhang, Sinong Wang, Sneha Agarwal, Soji Sajuyigbe, Soumith Chintala, Stephanie Max, Stephen Chen, Steve Kehoe, Steve Satterfield, Sudarshan Govindaprasad, Sumit Gupta, Summer Deng, Sungmin Cho, Sunny Virk, Suraj Subramanian, Sy Choudhury, Sydney Goldman, Tal Remez, Tamar Glaser, Tamara Best, Thilo Koehler, Thomas Robinson, Tianhe Li, Tianjun Zhang, Tim Matthews, Timothy Chou, Tzook Shaked, Varun Vontimitta, Victoria Ajayi, Victoria Montanez, Vijai Mohan, Vinay Satish Kumar, Vishal Mangla, Vlad Ionescu, Vlad Poenaru, Vlad Tiberiu Mihailescu, Vladimir Ivanov, Wei Li, Wenchen Wang, Wenwen Jiang, Wes Bouaziz, Will Constable, Xiaocheng Tang, Xiaojian Wu, Xiaolan Wang, Xilun Wu, Xinbo Gao, Yaniv Kleinman, Yanjun Chen, Ye Hu, Ye Jia, Ye Qi, Yenda Li, Yilin Zhang, Ying Zhang, Yossi Adi, Youngjin Nam, Yu, Wang, Yu Zhao, Yuchen Hao, Yundi Qian, Yunlu Li, Yuzi He, Zach Rait, Zachary DeVito, Zef Rosnbrick, Zhaoduo Wen, Zhenyu Yang, Zhiwei Zhao, and Zhiyu Ma. The llama 3 herd of models, 2024. URL https://arxiv.org/abs/2407.21783.

Batu Guan, Yao Wan, Zhangqian Bi, Zheng Wang, Hongyu Zhang, Pan Zhou, and Lichao Sun. CodeIP: A grammar-guided multi-bit watermark for large language models of code. In Yaser Al-Onaizan, Mohit Bansal, and Yun-Nung Chen (eds.), *Findings of the Association for Computational Linguistics: EMNLP 2024*, pp. 9243–9258, Miami, Florida, USA, November 2024. Association for Computational Linguistics. doi: 10.18653/v1/2024.findings-emnlp.541. URL https://aclanthology.org/2024.findings-emnlp.541/.

Yuxuan Guo, Zhiliang Tian, Yiping Song, Tianlun Liu, Liang Ding, and Dongsheng Li. Context-aware watermark with semantic balanced green-red lists for large language models. In Yaser Al-Onaizan, Mohit Bansal, and Yun-Nung Chen (eds.), *Proceedings of the 2024 Conference on Empirical Methods in Natural Language Processing*, pp. 22633–22646, Miami, Florida, USA, November 2024. Association for Computational Linguistics. doi: 10.18653/v1/2024.emnlp-main.1260. URL https://aclanthology.org/2024.emnlp-main.1260/.

Zhiwei He, Binglin Zhou, Hongkun Hao, Aiwei Liu, Xing Wang, Zhaopeng Tu, Zhuosheng Zhang, and Rui Wang. Can watermarks survive translation? on the cross-lingual consistency of text watermark for large language models. In Lun-Wei Ku, Andre Martins, and Vivek Srikumar (eds.), *Proceedings of the 62nd Annual Meeting of the Association for Computational Linguistics (Volume 1: Long Papers)*, pp. 4115–4129, Bangkok, Thailand, August 2024. Association for Computational Linguistics. doi: 10.18653/v1/2024.acl-long.226. URL https://aclanthology.org/2024.acl-long.226/.

Karl Moritz Hermann, Tomáš Kočiský, Edward Grefenstette, Lasse Espeholt, Will Kay, Mustafa Suleyman, and Phil Blunsom. Teaching machines to read and comprehend. In *Proceedings of the*

29th International Conference on Neural Information Processing Systems - Volume 1, NIPS'15, pp. 1693–1701, Cambridge, MA, USA, 2015. MIT Press.

Zhengmian Hu, Lichang Chen, Xidong Wu, Yihan Wu, Hongyang Zhang, and Heng Huang. Unbiased watermark for large language models. In *The Twelfth International Conference on Learning Representations*, 2024. URL https://openreview.net/forum?id=uWVC5FVidc.

Mingjia Huo, Sai Ashish Somayajula, Youwei Liang, Ruisi Zhang, Farinaz Koushanfar, and Pengtao Xie. Token-specific watermarking with enhanced detectability and semantic coherence for large language models. In *Proceedings of the 41st International Conference on Machine Learning*, ICML'24. JMLR.org, 2024.

Ganesh Jawahar, Muhammad Abdul-Mageed, and Laks Lakshmanan, V.S. Automatic detection of machine generated text: A critical survey. In Donia Scott, Nuria Bel, and Chengqing Zong (eds.), *Proceedings of the 28th International Conference on Computational Linguistics*, pp. 2296–2309, Barcelona, Spain (Online), December 2020. International Committee on Computational Linguistics. doi: 10.18653/v1/2020.coling-main.208. URL https://aclanthology.org/2020.coling-main.208/.

John Kirchenbauer, Jonas Geiping, Yuxin Wen, Jonathan Katz, Ian Miers, and Tom Goldstein. A watermark for large language models, 2024. URL https://arxiv.org/abs/2301.10226.

Rohith Kuditipudi, John Thickstun, Tatsunori Hashimoto, and Percy Liang. Robust distortion-free watermarks for language models. *Transactions on Machine Learning Research*, 2024. ISSN 2835-8856. URL https://openreview.net/forum?id=FpaCL1MO2C.

Taehyun Lee, Seokhee Hong, Jaewoo Ahn, Ilgee Hong, Hwaran Lee, Sangdoo Yun, Jamin Shin, and Gunhee Kim. Who wrote this code? watermarking for code generation. In Lun-Wei Ku, Andre Martins, and Vivek Srikumar (eds.), *Proceedings of the 62nd Annual Meeting of the Association for Computational Linguistics (Volume 1: Long Papers)*, pp. 4890–4911, Bangkok, Thailand, August 2024. Association for Computational Linguistics. doi: 10.18653/v1/2024.acl-long.268. URL https://aclanthology.org/2024.acl-long.268/.

Chin-Yew Lin. ROUGE: A package for automatic evaluation of summaries. In *Text Summarization Branches Out*, pp. 74–81, Barcelona, Spain, July 2004. Association for Computational Linguistics. URL https://aclanthology.org/W04-1013/.

Aiwei Liu, Leyi Pan, Xuming Hu, Shuang Li, Lijie Wen, Irwin King, and Philip S. Yu. An unforgeable publicly verifiable watermark for large language models. In *The Twelfth International Conference on Learning Representations*, 2024a. URL https://openreview.net/forum?id=gMLQwKDY3N.

Aiwei Liu, Leyi Pan, Yijian Lu, Jingjing Li, Xuming Hu, Xi Zhang, Lijie Wen, Irwin King, Hui Xiong, and Philip Yu. A survey of text watermarking in the era of large language models. *ACM Comput. Surv.*, 57(2), November 2024b. ISSN 0360-0300. doi: 10.1145/3691626. URL https://doi.org/10.1145/3691626.

Yepeng Liu and Yuheng Bu. Adaptive text watermark for large language models. In *Proceedings of the 41st International Conference on Machine Learning*, ICML'24. JMLR.org, 2024.

Yijian Lu, Aiwei Liu, Dianzhi Yu, Jingjing Li, and Irwin King. An entropy-based text watermarking detection method. In Lun-Wei Ku, Andre Martins, and Vivek Srikumar (eds.), *Proceedings of the 62nd Annual Meeting of the Association for Computational Linguistics (Volume 1: Long Papers)*, pp. 11724–11735, Bangkok, Thailand, August 2024. Association for Computational Linguistics. doi: 10.18653/v1/2024.acl-long.630. URL https://aclanthology.org/2024.acl-long.630/.

Eric Mitchell, Yoonho Lee, Alexander Khazatsky, Christopher D. Manning, and Chelsea Finn. Detectgpt: zero-shot machine-generated text detection using probability curvature. In *Proceedings of the 40th International Conference on Machine Learning*, ICML'23. JMLR.org, 2023.

OpenAI, Josh Achiam, Steven Adler, Sandhini Agarwal, Lama Ahmad, Ilge Akkaya, Florencia Leoni Aleman, Diogo Almeida, Janko Altenschmidt, Sam Altman, Shyamal Anadkat, Red Avila, Igor Babuschkin, Suchir Balaji, Valerie Balcom, Paul Baltescu, Haiming Bao, Mohammad Bavarian, Jeff Belgum, Irwan Bello, Jake Berdine, Gabriel Bernadett-Shapiro, Christopher Berner, Lenny Bogdonoff, Oleg Boiko, Madelaine Boyd, Anna-Luisa Brakman, Greg Brockman, Tim Brooks, Miles Brundage, Kevin Button, Trevor Cai, Rosie Campbell, Andrew Cann, Brittany Carey, Chelsea Carlson, Rory Carmichael, Brooke Chan, Che Chang, Fotis Chantzis, Derek Chen, Sully Chen, Ruby Chen, Jason Chen, Mark Chen, Ben Chess, Chester Cho, Casey Chu, Hyung Won Chung, Dave Cummings, Jeremiah Currier, Yunxing Dai, Cory Decareaux, Thomas Degry, Noah Deutsch, Damien Deville, Arka Dhar, David Dohan, Steve Dowling, Sheila Dunning, Adrien Ecoffet, Atty Eleti, Tyna Eloundou, David Farhi, Liam Fedus, Niko Felix, Simón Posada Fishman, Juston Forte, Isabella Fulford, Leo Gao, Elie Georges, Christian Gibson, Vik Goel, Tarun Gogineni, Gabriel Goh, Rapha Gontijo-Lopes, Jonathan Gordon, Morgan Grafstein, Scott Gray, Ryan Greene, Joshua Gross, Shixiang Shane Gu, Yufei Guo, Chris Hallacy, Jesse Han, Jeff Harris, Yuchen He, Mike Heaton, Johannes Heidecke, Chris Hesse, Alan Hickey, Wade Hickey, Peter Hoeschele, Brandon Houghton, Kenny Hsu, Shengli Hu, Xin Hu, Joost Huizinga, Shantanu Jain, Shawn Jain, Joanne Jang, Angela Jiang, Roger Jiang, Haozhun Jin, Denny Jin, Shino Jomoto, Billie Jonn, Heewoo Jun, Tomer Kaftan, Łukasz Kaiser, Ali Kamali, Ingmar Kanitscheider, Nitish Shirish Keskar, Tabarak Khan, Logan Kilpatrick, Jong Wook Kim, Christina Kim, Yongjik Kim, Jan Hendrik Kirchner, Jamie Kiros, Matt Knight, Daniel Kokotajlo, Łukasz Kondraciuk, Andrew Kondrich, Aris Konstantinidis, Kyle Kosic, Gretchen Krueger, Vishal Kuo, Michael Lampe, Ikai Lan, Teddy Lee, Jan Leike, Jade Leung, Daniel Levy, Chak Ming Li, Rachel Lim, Molly Lin, Stephanie Lin, Mateusz Litwin, Theresa Lopez, Ryan Lowe, Patricia Lue, Anna Makanju, Kim Malfacini, Sam Manning, Todor Markov, Yaniv Markovski, Bianca Martin, Katie Mayer, Andrew Mayne, Bob McGrew, Scott Mayer McKinney, Christine McLeavey, Paul McMillan, Jake McNeil, David Medina, Aalok Mehta, Jacob Menick, Luke Metz, Andrey Mishchenko, Pamela Mishkin, Vinnie Monaco, Evan Morikawa, Daniel Mossing, Tong Mu, Mira Murati, Oleg Murk, David Mély, Ashvin Nair, Reiichiro Nakano, Rajeev Nayak, Arvind Neelakantan, Richard Ngo, Hyeonwoo Noh, Long Ouyang, Cullen O'Keefe, Jakub Pachocki, Alex Paino, Joe Palermo, Ashley Pantuliano, Giambattista Parascandolo, Joel Parish, Emy Parparita, Alex Passos, Mikhail Pavlov, Andrew Peng, Adam Perelman, Filipe de Avila Belbute Peres, Michael Petrov, Henrique Ponde de Oliveira Pinto, Michael, Pokorny, Michelle Pokrass, Vitchyr H. Pong, Tolly Powell, Alethea Power, Boris Power, Elizabeth Proehl, Raul Puri, Alec Radford, Jack Rae, Aditya Ramesh, Cameron Raymond, Francis Real, Kendra Rimbach, Carl Ross, Bob Rotsted, Henri Roussez, Nick Ryder, Mario Saltarelli, Ted Sanders, Shibani Santurkar, Girish Sastry, Heather Schmidt, David Schnurr, John Schulman, Daniel Selsam, Kyla Sheppard, Toki Sherbakov, Jessica Shieh, Sarah Shoker, Pranav Shyam, Szymon Sidor, Eric Sigler, Maddie Simens, Jordan Sitkin, Katarina Slama, Ian Sohl, Benjamin Sokolowsky, Yang Song, Natalie Staudacher, Felipe Petroski Such, Natalie Summers, Ilya Sutskever, Jie Tang, Nikolas Tezak, Madeleine B. Thompson, Phil Tillet, Amin Tootoonchian, Elizabeth Tseng, Preston Tuggle, Nick Turley, Jerry Tworek, Juan Felipe Cerón Uribe, Andrea Vallone, Arun Vijayvergiya, Chelsea Voss, Carroll Wainwright, Justin Jay Wang, Alvin Wang, Ben Wang, Jonathan Ward, Jason Wei, CJ Weinmann, Akila Welihinda, Peter Welinder, Jiayi Weng, Lilian Weng, Matt Wiethoff, Dave Willner, Clemens Winter, Samuel Wolrich, Hannah Wong, Lauren Workman, Sherwin Wu, Jeff Wu, Michael Wu, Kai Xiao, Tao Xu, Sarah Yoo, Kevin Yu, Qiming Yuan, Wojciech Zaremba, Rowan Zellers, Chong Zhang, Marvin Zhang, Shengjia Zhao, Tianhao Zheng, Juntang Zhuang, William Zhuk, and Barret Zoph. Gpt-4 technical report, 2024. URL https://arxiv.org/abs/2303.08774.

Long Ouyang, Jeff Wu, Xu Jiang, Diogo Almeida, Carroll L. Wainwright, Pamela Mishkin, Chong Zhang, Sandhini Agarwal, Katarina Slama, Alex Ray, John Schulman, Jacob Hilton, Fraser Kelton, Luke Miller, Maddie Simens, Amanda Askell, Peter Welinder, Paul Christiano, Jan Leike, and Ryan Lowe. Training language models to follow instructions with human feedback. In *Proceedings of the 36th International Conference on Neural Information Processing Systems*, NIPS '22, Red Hook, NY, USA, 2022. Curran Associates Inc. ISBN 9781713871088.

Leyi Pan, Aiwei Liu, Zhiwei He, Zitian Gao, Xuandong Zhao, Yijian Lu, Binglin Zhou, Shuliang Liu, Xuming Hu, Lijie Wen, Irwin King, and Philip S. Yu. MarkLLM: An open-source toolkit for LLM watermarking. In Delia Irazu Hernandez Farias, Tom Hope, and Manling Li (eds.), *Proceedings of the 2024 Conference on Empirical Methods in Natural Language Processing: System Demonstrations*, pp. 61–71, Miami, Florida, USA, November 2024. Association for Computational Linguistics. doi: 10.18653/v1/2024.emnlp-demo.7. URL https://aclanthology.org/2024.emnlp-demo.7/.

Qwen, :, An Yang, Baosong Yang, Beichen Zhang, Binyuan Hui, Bo Zheng, Bowen Yu, Chengyuan Li, Dayiheng Liu, Fei Huang, Haoran Wei, Huan Lin, Jian Yang, Jianhong Tu, Jianwei Zhang, Jianxin Yang, Jiaxi Yang, Jingren Zhou, Junyang Lin, Kai Dang, Keming Lu, Keqin Bao, Kexin Yang, Le Yu, Mei Li, Mingfeng Xue, Pei Zhang, Qin Zhu, Rui Men, Runji Lin, Tianhao Li, Tianyi Tang, Tingyu Xia, Xingzhang Ren, Xuancheng Ren, Yang Fan, Yang Su, Yichang Zhang, Yu Wan, Yuqiong Liu, Zeyu Cui, Zhenru Zhang, and Zihan Qiu. Qwen2.5 technical report, 2025. URL https://arxiv.org/abs/2412.15115.

Alec Radford, Jong Wook Kim, Tao Xu, Greg Brockman, Christine McLeavey, and Ilya Sutskever. Robust speech recognition via large-scale weak supervision, 2022. URL https://arxiv.org/abs/2212.04356.

Jie Ren, Han Xu, Yiding Liu, Yingqian Cui, Shuaiqiang Wang, Dawei Yin, and Jiliang Tang. A robust semantics-based watermark for large language model against paraphrasing. In Kevin Duh, Helena Gomez, and Steven Bethard (eds.), *Findings of the Association for Computational Linguistics: NAACL 2024*, pp. 613–625, Mexico City, Mexico, June 2024. Association for Computational Linguistics. doi: 10.18653/v1/2024.findings-naacl.40. URL https://aclanthology.org/2024.findings-naacl.40/.

Freda Shi, Mirac Suzgun, Markus Freitag, Xuezhi Wang, Suraj Srivats, Soroush Vosoughi, Hyung Won Chung, Yi Tay, Sebastian Ruder, Denny Zhou, Dipanjan Das, and Jason Wei. Language models are multilingual chain-of-thought reasoners, 2022. URL https://arxiv.org/abs/2210.03057.

Ilia Shumailov, Zakhar Shumaylov, Yiren Zhao, Yarin Gal, Nicolas Papernot, and Ross Anderson. The curse of recursion: Training on generated data makes models forget, 2024. URL https://arxiv.org/abs/2305.17493.

Chris Stokel-Walker. Ai bot chatgpt writes smart essays - should professors worry? *Nature*, 2022. URL https://api.semanticscholar.org/CorpusID:254530623.

Yuki Takezawa, Ryoma Sato, Han Bao, Kenta Niwa, and Makoto Yamada. Necessary and sufficient watermark for large language models, 2025. URL https://arxiv.org/abs/2310.00833.

Hugo Touvron, Louis Martin, Kevin Stone, Peter Albert, Amjad Almahairi, Yasmine Babaei, Nikolay Bashlykov, Soumya Batra, Prajjwal Bhargava, Shruti Bhosale, Dan Bikel, Lukas Blecher, Cristian Canton Ferrer, Moya Chen, Guillem Cucurull, David Esiobu, Jude Fernandes, Jeremy Fu, Wenyin Fu, Brian Fuller, Cynthia Gao, Vedanuj Goswami, Naman Goyal, Anthony Hartshorn, Saghar Hosseini, Rui Hou, Hakan Inan, Marcin Kardas, Viktor Kerkez, Madian Khabsa, Isabel Kloumann, Artem Korenev, Punit Singh Koura, Marie-Anne Lachaux, Thibaut Lavril, Jenya Lee, Diana Liskovich, Yinghai Lu, Yuning Mao, Xavier Martinet, Todor Mihaylov, Pushkar Mishra, Igor Molybog, Yixin Nie, Andrew Poulton, Jeremy Reizenstein, Rashi Rungta, Kalyan Saladi, Alan Schelten, Ruan Silva, Eric Michael Smith, Ranjan Subramanian, Xiaoqing Ellen Tan, Binh Tang, Ross Taylor, Adina Williams, Jian Xiang Kuan, Puxin Xu, Zheng Yan, Iliyan Zarov, Yuchen Zhang, Angela Fan, Melanie Kambadur, Sharan Narang, Aurelien Rodriguez, Robert Stojnic, Sergey Edunov, and Thomas Scialom. Llama 2: Open foundation and fine-tuned chat models, 2023. URL https://arxiv.org/abs/2307.09288.

Christoforos Vasilatos, Manaar Alam, Talal Rahwan, Yasir Zaki, and Michail Maniatakos. Howkgpt: Investigating the detection of chatgpt-generated university student homework through context-aware perplexity analysis, 2025. URL https://arxiv.org/abs/2305.18226.

Zongqi Wang, Tianle Gu, Baoyuan Wu, and Yujiu Yang. MorphMark: Flexible adaptive watermarking for large language models. In Wanxiang Che, Joyce Nabende, Ekaterina Shutova, and Mohammad Taher Pilehvar (eds.), *Proceedings of the 63rd Annual Meeting of the Association for Computational Linguistics (Volume 1: Long Papers)*, pp. 4842–4860, Vienna, Austria, July 2025.

Association for Computational Linguistics. ISBN 979-8-89176-251-0. doi: 10.18653/v1/2025.acl-long.240. URL https://aclanthology.org/2025.acl-long.240/.

Bram Wouters. Optimizing watermarks for large language models. In Ruslan Salakhutdinov, Zico Kolter, Katherine Heller, Adrian Weller, Nuria Oliver, Jonathan Scarlett, and Felix Berkenkamp (eds.), *Proceedings of the 41st International Conference on Machine Learning*, volume 235 of *Proceedings of Machine Learning Research*, pp. 53251–53269. PMLR, 21–27 Jul 2024. URL https://proceedings.mlr.press/v235/wouters24a.html.

Qilong Wu and Varun Chandrasekaran. Bypassing LLM watermarks with color-aware substitutions. In Lun-Wei Ku, Andre Martins, and Vivek Srikumar (eds.), *Proceedings of the 62nd Annual Meeting of the Association for Computational Linguistics (Volume 1: Long Papers)*, pp. 8549–8581, Bangkok, Thailand, August 2024. Association for Computational Linguistics. doi: 10.18653/v1/2024.acl-long.464. URL https://aclanthology.org/2024.acl-long.464/.

Yihan Wu, Zhengmian Hu, Junfeng Guo, Hongyang Zhang, and Heng Huang. A resilient and accessible distribution-preserving watermark for large language models. In *Proceedings of the 41st International Conference on Machine Learning*, ICML'24. JMLR.org, 2024.

Linting Xue, Noah Constant, Adam Roberts, Mihir Kale, Rami Al-Rfou, Aditya Siddhant, Aditya Barua, and Colin Raffel. mT5: A massively multilingual pre-trained text-to-text transformer. In Kristina Toutanova, Anna Rumshisky, Luke Zettlemoyer, Dilek Hakkani-Tur, Iz Beltagy, Steven Bethard, Ryan Cotterell, Tanmoy Chakraborty, and Yichao Zhou (eds.), *Proceedings of the 2021 Conference of the North American Chapter of the Association for Computational Linguistics: Human Language Technologies*, pp. 483–498, Online, June 2021. Association for Computational Linguistics. doi: 10.18653/v1/2021.naacl-main.41. URL https://aclanthology.org/2021.naacl-main.41/.

An Yang, Anfeng Li, Baosong Yang, Beichen Zhang, Binyuan Hui, Bo Zheng, Bowen Yu, Chang Gao, Chengen Huang, Chenxu Lv, Chujie Zheng, Dayiheng Liu, Fan Zhou, Fei Huang, Feng Hu, Hao Ge, Haoran Wei, Huan Lin, Jialong Tang, Jian Yang, Jianhong Tu, Jianwei Zhang, Jianxin Yang, Jiaxi Yang, Jing Zhou, Jingren Zhou, Junyang Lin, Kai Dang, Keqin Bao, Kexin Yang, Le Yu, Lianghao Deng, Mei Li, Mingfeng Xue, Mingze Li, Pei Zhang, Peng Wang, Qin Zhu, Rui Men, Ruize Gao, Shixuan Liu, Shuang Luo, Tianhao Li, Tianyi Tang, Wenbiao Yin, Xingzhang Ren, Xinyu Wang, Xinyu Zhang, Xuancheng Ren, Yang Fan, Yang Su, Yichang Zhang, Yinger Zhang, Yu Wan, Yuqiong Liu, Zekun Wang, Zeyu Cui, Zhenru Zhang, Zhipeng Zhou, and Zihan Qiu. Qwen3 technical report, 2025. URL https://arxiv.org/abs/2505.09388.

Rowan Zellers, Ari Holtzman, Hannah Rashkin, Yonatan Bisk, Ali Farhadi, Franziska Roesner, and Yejin Choi. *Defending against neural fake news*. Curran Associates Inc., Red Hook, NY, USA, 2019.

Susan Zhang, Stephen Roller, Naman Goyal, Mikel Artetxe, Moya Chen, Shuohui Chen, Christopher Dewan, Mona Diab, Xian Li, Xi Victoria Lin, Todor Mihaylov, Myle Ott, Sam Shleifer, Kurt Shuster, Daniel Simig, Punit Singh Koura, Anjali Sridhar, Tianlu Wang, and Luke Zettlemoyer. Opt: Open pre-trained transformer language models, 2022. URL https://arxiv.org/abs/2205.01068.

Tianyi Zhang, Varsha Kishore, Felix Wu, Kilian Q. Weinberger, and Yoav Artzi. Bertscore: Evaluating text generation with bert, 2020. URL https://arxiv.org/abs/1904.09675.

Xuandong Zhao, Prabhanjan Vijendra Ananth, Lei Li, and Yu-Xiang Wang. Provable robust watermarking for AI-generated text. In *The Twelfth International Conference on Learning Representations*, 2024. URL https://openreview.net/forum?id=SsmT8aO45L.

A PROOF

A.1 THE PROOF FOR LEMMA 1

Fix a step t. Define $G = \sum_{i \in \mathcal{V}_g} e^{\ell_i^t}$ and $R = \sum_{i \notin \mathcal{V}_g} e^{\ell_i^t}$. Adding a bias δ_t to green logits yields $\tilde{\ell}_i^t = \ell_i^t + \delta_t \mathbf{1}\{i \in \mathcal{V}_g\}$. The next-token probability under softmax is as follows:

$$p_t(i;\delta_t) = \frac{\exp(\tilde{\ell}_i^t)}{\sum_j \exp(\tilde{\ell}_j^t)} = \frac{\exp\big(\ell_i^t + \delta_t \mathbf{1}\{i \in \mathcal{V}_g\}\big)}{\sum_{j \in \mathcal{V}_g} \exp(\ell_j^t + \delta_t) \; + \; \sum_{j \in \mathcal{V}_r} \exp(\ell_j^t)} = \frac{\exp\big(\ell_i^t + \delta_t \, \mathbf{1}\{i \in \mathcal{V}_g\}\big)}{e^{\delta_t} G + R}, \tag{7}$$

After adding δ_t to green logits,

$$p_t^g(\delta_t) = \frac{e^{\delta_t} G}{e^{\delta_t} G + R}. \tag{8}$$

Differentiate:

$$\frac{\partial p_t^g(\delta_t)}{\partial \delta_t} = \frac{e^{\delta_t} G R}{(e^{\delta_t} G + R)^2}. \tag{9}$$

At $\delta_t = 0$, the derivative at 0 equals $\frac{GR}{(G+R)^2} = \frac{G}{G+R}\Big(1 - \frac{G}{G+R}\Big) = p_t^g(0)\big(1 - p_t^g(0)\big) \equiv \beta_t$.

A first-order Taylor expansion gives $p_t^g(\delta_t) \approx p_t^g(0) + \beta_t \delta_t$, i.e., $\Delta p_t^g \approx \beta_t \delta_t$.

A.2 THE PROOF FOR LEMMA 2 (KL CASE)

Fix a step t. Define $G = \sum_{i \in \mathcal{V}_g} e^{\ell_i^t}$ and $R = \sum_{i \notin \mathcal{V}_g} e^{\ell_i^t}$, $Z = G + R$, $p_t^g(0) = \frac{G}{Z}$, and $\beta_t = p_t^g(0)\big(1 - p_t^g(0)\big)$.

Let $p_t(i;0) = \frac{e^{\ell_i^t}}{Z}$ be the pre-bias next-token distribution and let $q_t(i;\delta_t) = \frac{e^{\ell_i^t + \delta_t \mathbf{1}\{i \in \mathcal{V}_g\}}}{e^{\delta_t} G + R}$ be the distribution after adding a green-only bias δ_t.

The per-step KL divergence is as follows:

$$\begin{aligned} \mathrm{KL}_t &= \sum_i p_t(i;0) \log \frac{p_t(i;0)}{q_t(i;\delta_t)} \\ &= \sum_i \frac{e^{\ell_i^t}}{Z} \Big[\big(\ell_i^t - \log Z\big) - \Big(\ell_i^t + \delta_t \mathbf{1}\{i \in \mathcal{V}_g\} - \log(e^{\delta_t} G + R)\Big) \Big] \\ &= \sum_i \frac{e^{\ell_i^t}}{Z} \Big[-\delta_t \mathbf{1}\{i \in \mathcal{V}_g\} + \log(e^{\delta_t} G + R) - \log Z \Big]. \end{aligned} \tag{10}$$

Using $\sum_i \frac{e^{\ell_i^t}}{Z} \, \mathbf{1}\{i \in \mathcal{V}_g\} = p_t^g(0) = G/Z$ and $\sum_i \frac{e^{\ell_i^t}}{Z} = 1$, this simplifies to the scalar function as follows:

$$\mathrm{KL}_t = -p_t^g(0)\delta_t + \log\Big(\frac{e^{\delta_t} G + R}{Z}\Big) = -\frac{G}{Z}\delta_t + \log\Big(\frac{e^{\delta_t} G + R}{G + R}\Big). \tag{11}$$

Define $D(\delta_t) := \frac{e^{\delta_t} G + R}{G + R} = \frac{G}{Z} e^{\delta_t} + \frac{R}{Z} = p_t^g(0) e^{\delta_t} + \big(1 - p_t^g(0)\big)$.

A second-order Taylor expansion and using $\log(1+x) = x - \frac{1}{2}x^2 + O(x^3)$, at $\delta_t = 0$ gives

$$\begin{gathered} D(\delta_t) = 1 + p_t^g(0)\delta_t + \tfrac{1}{2} p_t^g(0)\delta_t^2 + O(\delta_t^3) \\ \log D(\delta_t) = p_t^g(0)\delta_t + \tfrac{1}{2}\, p_t^g(0)\big(1 - p_t^g(0)\big)\, \delta_t^2 + O(\delta_t^3). \end{gathered} \tag{12}$$

Therefore

$$\mathrm{KL}_t = \underbrace{p_t^g(0)\delta_t - p_t^g(0)\delta_t}_{=0} + \tfrac{1}{2} p_t^g(0)\big(1 - p_t^g(0)\big)\delta_t^2 + O(\delta_t^3) = \tfrac{1}{2}\beta_t \delta_t^2 + O(\delta_t^3), \tag{13}$$

which shows that the local quadratic coefficient is $\kappa_t = \frac{1}{2}\beta_t > 0$.

A.3 The proof for Theorem 1

Let $\delta_t = \alpha\,\bar{m}_t$ with $\bar{m}_t \geq 0$, and define $S = \sum_t \beta_t\,\bar{m}_t \quad (\beta_t \geq 0), K = \sum_t \kappa_t\,\bar{m}_t^2 \quad (\kappa_t > 0)$. Then, the gain and cost surrogates become $G(\alpha) = \alpha S$ and $C(\alpha) = \alpha^2 K$, so the objective is as follows:

$$F_\omega(\alpha) = \omega\,S\,\alpha - K\,\alpha^2, \omega > 0. \tag{14}$$

Compute derivatives:

$$F'_\omega(\alpha) = \omega S - 2K\alpha, F''_\omega(\alpha) = -2K. \tag{15}$$

Since $K = \sum_t \kappa_t \bar{m}_t^2 > 0$, we have $F''_\omega(\alpha) = -2K < 0$, so F_ω is strictly concave in α. Setting $F'_\omega(\alpha) = 0$ gives the unique critical point $\alpha^* = \omega S/(2K)$, which is therefore the unique global maximizer. Moreover,

$$\frac{\partial \alpha^*}{\partial S} = \frac{\omega}{2K} > 0, \frac{\partial \alpha^*}{\partial K} = -\frac{\omega S}{2K^2} < 0, \tag{16}$$

showing that the optimal calibration increases with S and decreases with K.

Assumptions and scope. (i) Small-bias regime so that the first-/second-order expansions are accurate; (ii) linearity of expectation (or weak dependence) in the z-statistic's numerator; (iii) a fixed KGW partition; (iv) under a local KL proxy, $\kappa_t \simeq \frac{1}{2}\,\beta_t$ is common, which can make the reward–cost ratio $r_t = \beta_t/\kappa_t$ approximately constant; empirical comparisons then become especially informative.

A.4 Implementation Details

For the watermarking methods, we set the SWEET entropy threshold to 0.9. For UPV, we use a 16 bit-number and set σ to 0.01. For MorphMark, we use the exponential type with parameters k_{exp}=1.30 and p_0=0.15. Note that we extensively tuned MorphMark's hyper-parameters.

DynamicBias adds only two lightweight operations per step: (1) compute the certainty margin from the top-c logits and update the sequence-level average $\bar{m}_t$ (margin $O(c)$, update $O(1)$); (2) set the calibrated bias $\delta_t = \alpha\bar{m}_t$. No extra forward passes, gradients, or model-specific training are required.

B Additional Experiments

B.1 Overall Performance

Since the main text includes only results averaged over four LLMs, we provide per-model results. Tables 9 and 10 show the results on C4/mC4 and GSM8K/MGSM. We observe that integrating DynamicBias is effective across models.

B.2 Comparison to using an Auxiliary Model

We also compare DynamicBias with the auxiliary-model approach of TS (Huo et al., 2024), which is not model-independent. For a fair comparison, we employ the OPT-1.3B (Zhang et al., 2022) and Llama2-13B-Instruct (Touvron et al., 2023) models. Table 11 shows the results. Under the TS watermarking configuration with temperature=1 and top-k=50, DynamicBias consistently outperforms TS.

B.3 Effect of the pool size c

Since the main text includes only results averaged over languages, we provide per-language results. Table 12 shows the results on C4/mC4 and GSM8K/MGSM.

B.4 Sequence-Aware Calibration

Since the main text includes only results averaged over languages, we provide per-language results. Table 13 shows the results on C4/mC4 and GSM8K/MGSM using Qwen3-4B. We observed that

Table 9: Performance of each method on C4 and mC4 across languages with averaged scores (AVG).

Model	Method	EN			KR			JA			AVG		
		PPL	AUC	TPR@5	PPL	AUC	TPR@5	PPL	AUC	TPR@5	PPL	AUC	TPR@5
Llama3.2 -3B	Un-Water	3.49	-	-	3.86	-	-	4.53	-	-	3.96	-	-
	KGW	5.83	0.996	0.990	7.48	0.987	0.966	7.76	0.988	0.968	7.02	0.990	0.975
	Unigram	6.55	0.998	0.996	4.86	0.988	0.962	6.76	0.995	0.986	6.06	0.994	0.981
	UPV	5.36	1.000	0.998	5.70	0.960	0.858	6.31	0.968	0.924	5.79	0.976	0.926
	SWEET	5.25	0.996	0.990	7.07	0.989	0.966	7.28	0.989	0.972	6.53	0.991	0.976
	MorphMark	3.62	0.974	0.852	4.65	0.898	0.672	4.87	0.899	0.650	4.38	0.924	0.725
	KGW+D	**4.62**	**0.999**	**0.996**	**6.02**	**0.990**	**0.968**	**6.62**	**0.989**	**0.968**	**5.75**	**0.993**	**0.977**
	Unigram+D	**4.72**	**1.000**	**0.998**	5.15	**0.989**	**0.966**	**6.34**	0.991	0.968	**5.40**	0.993	0.977
	UPV+D	**4.50**	0.998	0.992	**5.42**	0.947	0.784	**6.04**	0.960	0.884	**5.32**	0.968	0.886
Qwen2.5 -3B	Un-Water	3.93	-	-	3.30	-	-	3.26	-	-	3.50	-	-
	KGW	8.96	0.992	0.982	7.22	0.968	0.930	7.24	0.989	0.976	7.81	0.983	0.962
	Unigram	8.03	0.990	0.964	6.55	0.955	0.892	7.18	0.980	0.960	7.25	0.975	0.939
	UPV	7.82	0.991	0.978	5.56	0.943	0.874	5.62	0.975	0.950	6.33	0.970	0.934
	SWEET	8.28	0.988	0.974	6.27	0.949	0.904	6.46	0.979	0.954	7.00	0.972	0.944
	MorphMark	4.29	0.968	0.952	3.41	0.887	0.724	3.48	0.914	0.762	3.73	0.923	0.813
	KGW+D	**5.02**	**0.999**	**0.998**	**4.97**	**0.990**	**0.970**	**5.19**	**0.995**	**0.986**	**5.06**	**0.995**	**0.985**
	Unigram+D	**4.86**	**0.995**	**0.980**	**4.81**	**0.984**	**0.960**	**5.17**	**0.984**	**0.966**	**4.95**	**0.987**	**0.969**
	UPV+D	**4.95**	**0.997**	**0.990**	**4.65**	**0.974**	**0.904**	**4.72**	**0.985**	**0.954**	**4.77**	**0.985**	**0.949**
Qwen3 -1.7B	Un-Water	5.11	-	-	3.80	-	-	4.06	-	-	4.32	-	-
	KGW	5.99	0.979	0.960	5.10	0.906	0.830	5.67	0.929	0.868	5.59	0.938	0.886
	Unigram	5.96	0.976	0.942	4.40	0.940	0.856	5.09	0.945	0.798	5.15	0.954	0.865
	UPV	5.98	0.985	0.952	4.55	0.892	0.760	5.05	0.897	0.766	5.19	0.925	0.826
	SWEET	5.65	0.977	0.940	4.73	0.910	0.824	5.19	0.919	0.844	5.19	0.935	0.869
	MorphMark	5.19	0.899	0.584	3.79	0.839	0.454	3.98	0.804	0.724	4.32	0.847	0.587
	KGW+D	6.25	**0.988**	**0.970**	5.15	**0.956**	**0.906**	5.89	**0.966**	**0.928**	5.76	**0.970**	**0.935**
	Unigram+D	6.03	**0.982**	**0.952**	4.57	**0.961**	**0.884**	5.37	**0.967**	**0.892**	5.32	**0.970**	**0.909**
	UPV+D	6.13	**0.991**	**0.956**	4.82	**0.943**	**0.858**	5.36	**0.934**	**0.842**	5.44	**0.956**	**0.885**
Qwen3 -4B	Un-Water	4.48	-	-	4.27	-	-	4.7	-	-	4.48	-	-
	KGW	5.29	0.997	0.994	5.55	0.978	0.950	6.31	0.977	0.962	5.72	0.984	0.969
	Unigram	5.26	0.995	0.990	5.29	0.984	0.948	5.70	0.964	0.824	5.42	0.981	0.921
	UPV	5.27	0.991	0.984	5.26	0.953	0.880	5.65	0.929	0.806	5.39	0.958	0.890
	SWEET	4.90	0.997	0.980	5.09	0.984	0.960	5.77	0.978	0.946	5.25	0.986	0.962
	MorphMark	4.5	0.895	0.522	4.33	0.898	0.542	4.88	0.865	0.456	4.57	0.886	0.507
	KGW+D	5.38	**0.998**	**0.996**	5.59	**0.994**	**0.984**	6.39	**0.990**	**0.990**	5.79	**0.994**	**0.990**
	Unigram+D	5.31	**0.997**	**0.996**	5.34	**0.986**	**0.952**	6.10	**0.971**	**0.850**	5.58	**0.985**	**0.933**
	UPV+D	5.34	**0.995**	**0.996**	**5.26**	**0.979**	**0.942**	5.78	**0.963**	**0.866**	5.46	**0.979**	**0.935**

sequence-aware calibration delivers higher detectability across languages than the token-level variant. Figure 6 presents the parameter-tuning results for MorphMark.

B.5 Number of Green Tokens Generated

Table 14 shows the average number of green tokens on C4 and GSM8K using Qwen3-4B. Because WordSub replaces words using WordNet, it often increases the total token count; accordingly, counts are higher under this attack. We also observe that applying DynamicBias increases the number of green tokens generated.

B.6 Decoding Strategy

We provide per-model results. Tables 15 and 16 show the results on C4/mC4 and GSM8K/MGSM using top-p decoding strategy with temperature.

Table 10: Performance of each method on GSM8K and MGSM across languages with averaged scores (AVG).

Model	Method	EN			KR			JA			AVG		
		ACC	AUC	TPR@5	ACC	AUC	TPR@5	ACC	AUC	TPR@5	ACC	AUC	TPR@5
Llama3.2 -3B	Un-Water	71.95	-	-	7.28	-	-	8.57	-	-	29.27	-	-
	KGW	64.06	0.963	0.814	6.29	0.982	0.900	6.44	0.985	0.920	25.60	0.980	0.878
	Unigram	61.64	0.938	0.724	6.44	0.960	0.828	6.75	0.970	0.860	24.94	0.960	0.804
	UPV	61.41	0.927	0.702	5.61	0.932	0.748	7.35	0.929	0.728	24.79	0.930	0.726
	SWEET	67.75	0.920	0.697	6.67	0.989	0.952	6.82	0.987	0.912	27.08	0.970	0.854
	MorphMark	72.25	0.750	0.253	7.43	0.745	0.272	9.17	0.786	0.368	29.62	0.760	0.298
	KGW+D	59.97	**0.982**	**0.900**	6.07	**0.989**	**0.948**	**7.20**	**0.988**	**0.944**	24.41	**0.990**	**0.931**
	Unigram+D	58.15	**0.980**	**0.906**	6.07	**0.987**	**0.916**	6.29	**0.979**	**0.876**	23.50	**0.980**	**0.899**
	UPV+D	57.09	**0.977**	**0.888**	**5.84**	**0.967**	**0.848**	5.76	**0.968**	**0.864**	22.90	**0.970**	**0.867**
Qwen2.5 -3B	Un-Water	33.06	-	-	9.25	-	-	7.51	-	-	16.61	-	-
	KGW	32.37	0.909	0.649	6.29	0.977	0.864	7.58	0.986	0.920	15.41	0.960	0.811
	Unigram	29.11	0.908	0.611	6.90	0.956	0.720	6.90	0.979	0.912	14.30	0.950	0.748
	UPV	29.11	0.856	0.477	5.91	0.958	0.756	5.91	0.934	0.736	13.64	0.920	0.715
	SWEET	34.57	0.898	0.590	6.82	0.994	0.972	7.51	0.990	0.948	16.30	0.960	0.837
	MorphMark	35.94	0.722	0.227	7.88	0.840	0.504	7.05	0.835	0.400	16.96	0.799	0.377
	KGW+D	31.01	**0.973**	**0.883**	**6.60**	0.974	**0.872**	**7.96**	0.972	0.880	15.19	**0.970**	**0.878**
	Unigram+D	27.14	**0.963**	**0.822**	**7.66**	0.918	0.572	**6.90**	0.955	0.768	13.90	**0.950**	0.721
	UPV+D	26.76	**0.956**	**0.788**	**6.29**	0.952	0.732	**6.52**	**0.938**	**0.748**	13.19	**0.950**	**0.756**
Qwen3 -1.7B	Un-Water	64.67	-	-	9.33	-	-	9.1	-	-	27.70	-	-
	KGW	62.55	0.696	0.198	8.64	0.780	0.284	8.57	0.774	0.336	26.59	0.750	0.273
	Unigram	63.08	0.711	0.208	8.64	0.749	0.232	8.26	0.829	0.388	26.66	0.760	0.276
	UPV	61.56	0.686	0.195	8.49	0.703	0.188	7.81	0.730	0.188	25.95	0.710	0.190
	SWEET	64.44	0.576	0.096	8.79	0.715	0.216	8.72	0.758	0.268	27.32	0.680	0.193
	MorphMark	65.35	0.576	0.086	8.87	0.604	0.136	8.42	0.644	0.108	27.55	0.608	0.110
	KGW+D	60.88	**0.935**	**0.700**	8.11	**0.931**	**0.716**	**9.02**	**0.928**	**0.668**	26.00	**0.930**	**0.695**
	Unigram+D	**63.68**	**0.926**	**0.682**	**8.64**	**0.871**	**0.520**	8.04	**0.928**	**0.700**	**26.79**	**0.910**	**0.634**
	UPV+D	56.33	**0.902**	**0.644**	7.35	**0.845**	**0.384**	**8.19**	**0.867**	**0.472**	23.96	**0.870**	**0.500**
Qwen3 -4B	Un-Water	55.42	-	-	11.68	-	-	10.39	-	-	25.83	-	-
	KGW	54.89	0.824	0.404	11.52	0.705	0.200	10.54	0.794	0.388	25.65	0.770	0.331
	Unigram	56.03	0.699	0.162	9.70	0.761	0.340	10.16	0.779	0.328	25.30	0.750	0.277
	UPV	56.41	0.669	0.175	11.37	0.639	0.156	9.78	0.743	0.276	25.85	0.680	0.202
	SWEET	47.46	0.694	0.202	11.60	0.685	0.184	10.39	0.718	0.260	23.15	0.700	0.215
	MorphMark	56.48	0.604	0.096	11.37	0.574	0.100	10.77	0.638	0.148	26.21	0.605	0.115
	KGW+D	53.90	**0.974**	**0.861**	**11.68**	**0.904**	**0.560**	9.70	**0.941**	**0.708**	25.09	**0.940**	**0.710**
	Unigram+D	55.88	**0.916**	**0.631**	**10.84**	**0.857**	**0.508**	9.86	**0.902**	**0.652**	**25.53**	**0.890**	**0.597**
	UPV+D	51.25	**0.900**	**0.621**	10.84	**0.817**	**0.404**	9.25	**0.886**	**0.592**	23.78	**0.870**	**0.539**

C Experimental details

We evaluate on two additional datasets beyond PPL. For CNN/DailyMail (CNN/DM), we randomly sample 250 instances from the test dataset. For HumanEval, we use 164 coding problems.

D Limitations

DynamicBias is training-free and detector-compatible. The remaining limits are pragmatic. (1) Theory uses a small-bias surrogate. Empirically, the trend persists beyond that regime. (2) We rely on top-k log-probabilities, which are widely available. When k is small or unavailable, we can use an entropy proxy. (3) We focus on common edits and paraphrases. Fully adaptive margin-shaping attacks are left for future work. (4) Very large models and niche domains are not exhaustively covered. Pilot checks show similar tendencies.

Table 11: Comparison to using an auxiliary model.

OPT 1.3B			**Llama2 13B**		
Method	PPL	AUC	Method	PPL	AUC
Un-Water	12.32	-	Un-Water	6.16	-
KGW	22.84	0.998	KGW	12.30	0.997
Unigram	19.99	**0.999**	Unigram	12.16	**0.998**
UPV	11.56	0.994	UPV	8.16	0.993
TS	14.90	0.996	TS	7.62	**0.998**
KGW + D	**13.48**	0.994	KGW + D	**7.57**	0.997
Unigram + D	**14.09**	0.993	Unigram + D	**7.58**	0.994
UPV + D	**11.41**	0.965	UPV + D	**6.43**	0.957

Table 12: Effect of the pool size c in the margin definition for each language.

c	C4 (EN)		mC4 (KR)		mC4 (JA)		GSM (EN)		MGSM (KR)		MGSM (JA)	
	PPL↓	AUC↑	PPL↓	AUC↑	PPL↓	AUC↑	ACC↑	AUC↑	ACC↑	AUC↑	ACC↑	AUC↑
2	**4.79**	0.993	**4.88**	0.982	**5.62**	0.975	49.73	0.919	11.52	0.841	**9.86**	0.889
5	5.38	0.998	5.59	0.994	6.39	0.990	**53.90**	0.974	**11.68**	0.904	9.70	0.941
10	5.99	**0.999**	6.37	**0.995**	7.19	**0.993**	**53.90**	**0.990**	10.92	**0.960**	9.55	**0.975**

Table 13: Performance of sequence-aware calibration and token-level DynamicBias for each language.

Scope	C4 (EN)		mC4 (KR)		mC4 (JA)		GSM (EN)		MGSM (KR)		MGSM (JA)	
	PPL	AUC	PPL	AUC	PPL	AUC	ACC	AUC	ACC	AUC	ACC	AUC
Morphmark ($k_{linear} = 1.55$)	**4.5**	0.8951	**4.33**	0.8980	4.88	0.8654	56.48	0.6042	11.37	0.5742	**10.77**	0.6375
Morphmark ($k_{linear} = 9.0$)	5.03	0.9935	5.44	0.9889	5.79	0.9748	56.25	0.7357	**11.75**	0.7237	10.16	0.7802
Token	4.69	0.9487	5.02	0.8646	**4.55**	0.8692	**57.7**	0.7944	11.68	0.6442	10.46	0.7096
Sequence	5.38	**0.9983**	5.59	**0.9942**	6.39	**0.9903**	53.9	**0.9736**	11.68	**0.9037**	9.7	**0.9414**

Table 14: Average number of green tokens across dataset.

Method	C4 (Green / Total)			GSM8K (Green / Total)		
	Original	WordDel	WordSub	Original	WordDel	WordSub
KGW	98.58 / 198.36	39.57 / 97.90	87.13 / 252.72	52.67 / 181.27	21.56 / 85.10	53.90 / 191.12
KGW+D	**100.93** / 198.67	**40.07** / 98.14	**87.92** / 253.06	**66.14** / 182.61	**24.75** / 85.89	**57.19** / 192.78

Table 15: Performance of each method on C4 and mC4 across languages with top-p sampling.

Model	Method	EN			KR			JA			AVG		
		PPL	AUC	TPR@5	PPL	AUC	TPR@5	PPL	AUC	TPR@5	PPL	AUC	TPR@5
Llama3.2 -3B	Un-Water	3.79	-	-	5.09	-	-	6.23	-	-	5.04	-	-
	KGW	6.77	0.997	0.992	11.52	0.989	0.976	11.53	0.995	0.976	9.94	0.994	0.982
	Unigram	7.64	0.998	0.996	7.00	0.995	0.978	10.27	0.996	0.992	8.30	0.997	0.989
	UPV	5.92	1.000	0.996	7.14	0.975	0.902	8.38	0.975	0.920	7.15	0.983	0.939
	SWEET	5.94	0.996	0.990	11.06	0.989	0.972	11.11	0.992	0.982	9.37	0.992	0.981
	MorphMark	3.90	0.977	0.886	5.99	0.905	0.716	6.40	0.916	0.680	5.43	0.932	0.761
	KGW+D	**5.05**	**1.000**	**0.998**	**8.87**	**0.993**	**0.982**	**9.28**	0.994	**0.984**	**7.73**	**0.996**	**0.988**
	Unigram+D	**5.21**	**0.999**	**0.996**	8.04	0.992	0.968	**9.81**	0.989	0.976	**7.69**	0.994	0.980
	UPV+D	**4.92**	0.999	0.988	7.41	0.945	0.776	**7.87**	0.961	0.864	**6.73**	0.968	0.876
Qwen2.5 -3B	Un-Water	4.75	-	-	3.77	-	-	3.81	-	-	4.11	-	-
	KGW	10.57	0.993	0.984	8.57	0.974	0.942	8.79	0.989	0.982	9.31	0.985	0.969
	Unigram	9.45	0.989	0.964	7.99	0.967	0.916	8.70	0.984	0.970	8.71	0.980	0.950
	UPV	9.26	0.993	0.980	6.53	0.947	0.886	6.60	0.982	0.960	7.46	0.974	0.942
	SWEET	9.57	0.989	0.972	7.47	0.950	0.908	7.66	0.980	0.958	8.23	0.973	0.946
	MorphMark	5.01	0.967	0.950	3.96	0.896	0.736	4.04	0.923	0.762	4.34	0.929	0.816
	KGW+D	**5.85**	**1.000**	**1.000**	**5.81**	**0.994**	**0.980**	**6.07**	**0.995**	**0.984**	**5.91**	**0.996**	**0.988**
	Unigram+D	**5.74**	**0.994**	**0.982**	**5.89**	**0.991**	**0.980**	**6.19**	**0.988**	**0.974**	**5.94**	**0.991**	**0.979**
	UPV+D	**5.98**	**0.996**	**0.992**	**5.31**	**0.977**	**0.936**	**5.50**	0.981	0.942	**5.60**	**0.985**	**0.957**
Qwen3 -1.7B	Un-Water	5.23	-	-	3.95	-	-	4.17	-	-	4.45	-	-
	KGW	6.17	0.979	0.950	5.50	0.908	0.824	6.04	0.936	0.884	5.90	0.941	0.886
	Unigram	6.15	0.977	0.942	5.02	0.942	0.870	5.51	0.947	0.806	5.56	0.955	0.873
	UPV	6.21	0.985	0.948	4.96	0.889	0.784	5.35	0.908	0.788	5.51	0.928	0.840
	SWEET	5.88	0.979	0.942	5.05	0.910	0.820	5.42	0.919	0.840	5.45	0.936	0.867
	MorphMark	5.28	0.896	0.542	3.96	0.840	0.462	4.15	0.803	0.482	4.46	0.847	0.495
	KGW+D	6.38	**0.990**	**0.976**	**5.46**	**0.960**	**0.910**	6.23	**0.970**	**0.944**	6.02	**0.973**	**0.943**
	Unigram+D	6.18	**0.978**	**0.942**	5.13	**0.961**	**0.876**	5.78	**0.968**	**0.894**	5.70	**0.969**	**0.904**
	UPV+D	6.32	**0.991**	**0.958**	5.12	**0.940**	**0.858**	5.77	**0.940**	**0.840**	5.74	**0.957**	**0.885**
Qwen3 -4B	Un-Water	4.54	-	-	4.41	-	-	4.96	-	-	4.64	-	-
	KGW	5.39	0.998	0.998	5.96	0.984	0.958	6.57	0.981	0.952	5.97	0.988	0.969
	Unigram	5.43	0.996	0.992	5.57	0.984	0.928	5.99	0.963	0.824	5.66	0.981	0.915
	UPV	5.30	0.992	0.990	5.44	0.953	0.878	5.96	0.933	0.822	5.57	0.959	0.897
	SWEET	4.97	0.996	0.982	5.48	0.988	0.966	6.00	0.980	0.936	5.48	0.988	0.961
	MorphMark	4.59	0.894	0.518	4.46	0.886	0.528	4.97	0.868	0.450	4.67	0.882	0.499
	KGW+D	5.44	**0.998**	0.996	**5.79**	**0.994**	**0.984**	**6.54**	**0.988**	**0.980**	**5.92**	**0.993**	**0.987**
	Unigram+D	5.46	**0.997**	**0.996**	5.62	**0.987**	**0.946**	6.35	**0.972**	**0.862**	5.81	**0.985**	**0.935**
	UPV+D	5.44	**0.994**	**0.994**	5.53	**0.973**	**0.926**	6.02	**0.954**	**0.856**	5.66	**0.974**	**0.925**

Table 16: Performance of each method on GSM and MGSM across languages with top-p sampling.

Model	Method	EN			KR			JA			AVG		
		ACC	AUC	TPR@5	ACC	AUC	TPR@5	ACC	AUC	TPR@5	ACC	AUC	TPR@5
Llama3.2 -3B	Un-Water	72.02	-	-	7.66	-	-	8.49	-	-	29.39	-	-
	KGW	61.71	0.961	0.817	6.22	0.984	0.924	6.14	0.985	0.908	24.69	0.977	0.883
	Unigram	60.12	0.939	0.718	5.69	0.975	0.872	6.14	0.975	0.868	23.98	0.963	0.819
	UPV	58.45	0.929	0.707	5.91	0.946	0.776	6.52	0.944	0.788	23.63	0.940	0.757
	SWEET	68.54	0.915	0.683	6.60	0.992	0.968	6.90	0.988	0.936	27.35	0.965	0.862
	MorphMark	70.96	0.742	0.263	7.28	0.740	0.240	9.10	0.768	0.312	29.11	0.750	0.272
	KGW+D	60.35	**0.980**	**0.890**	5.61	**0.992**	**0.968**	**6.37**	**0.994**	**0.984**	24.11	**0.989**	**0.947**
	Unigram+D	57.16	**0.982**	**0.917**	**5.91**	**0.991**	**0.960**	5.99	**0.983**	**0.908**	23.02	**0.985**	**0.928**
	UPV+D	54.44	**0.968**	**0.837**	**6.22**	**0.954**	**0.776**	**6.75**	**0.956**	**0.808**	22.47	**0.959**	**0.807**
Qwen2.5 -3B	Un-Water	34.12	-	-	8.79	-	-	7.58	-	-	16.83	-	-
	KGW	31.54	0.913	0.646	6.75	0.978	0.876	7.43	0.986	0.944	15.24	0.959	0.822
	Unigram	28.73	0.902	0.597	6.52	0.958	0.776	5.69	0.982	0.920	13.65	0.947	0.764
	UPV	29.26	0.856	0.487	5.46	0.959	0.780	6.52	0.943	0.776	13.75	0.919	0.681
	SWEET	33.21	0.895	0.604	7.20	0.993	0.952	6.97	0.991	0.944	15.79	0.960	0.833
	MorphMark	36.01	0.732	0.233	7.28	0.819	0.444	6.97	0.836	0.400	16.75	0.796	0.359
	KGW+D	30.48	**0.976**	**0.887**	6.67	**0.982**	**0.876**	**7.73**	0.978	0.904	14.96	**0.979**	**0.889**
	Unigram+D	26.61	**0.969**	**0.849**	**6.90**	0.917	0.576	**6.75**	0.969	0.856	13.42	**0.952**	0.760
	UPV+D	27.22	**0.937**	**0.709**	**6.07**	0.937	0.688	5.99	0.931	0.712	13.09	**0.935**	**0.703**
Qwen3 -1.7B	Un-Water	64.29	-	-	9.40	-	-	8.57	-	-	27.42	-	-
	KGW	62.62	0.699	0.204	9.10	0.783	0.320	8.72	0.781	0.352	26.81	0.754	0.292
	Unigram	63.23	0.711	0.211	8.72	0.741	0.260	8.34	0.843	0.420	26.76	0.765	0.297
	UPV	62.02	0.684	0.197	7.96	0.704	0.176	7.81	0.735	0.212	25.93	0.708	0.195
	SWEET	64.06	0.576	0.092	8.95	0.716	0.208	8.57	0.755	0.272	27.19	0.682	0.191
	MorphMark	64.22	0.576	0.090	8.87	0.600	0.120	8.64	0.642	0.100	27.24	0.606	0.103
	KGW+D	60.50	**0.936**	**0.697**	8.72	**0.929**	**0.700**	**9.02**	**0.930**	**0.688**	26.08	**0.931**	**0.695**
	Unigram+D	**63.23**	**0.926**	**0.676**	**9.17**	**0.874**	**0.508**	7.96	**0.926**	**0.656**	**26.79**	**0.909**	**0.613**
	UPV+D	57.01	**0.872**	**0.558**	7.13	**0.823**	**0.352**	**7.96**	**0.842**	**0.416**	24.03	**0.846**	**0.479**
Qwen3 -4B	Un-Water	55.27	-	-	11.52	-	-	10.46	-	-	25.75	-	-
	KGW	54.51	0.824	0.404	11.45	0.710	0.200	10.24	0.799	0.396	25.40	0.777	0.333
	Unigram	56.41	0.701	0.166	9.55	0.759	0.332	10.31	0.790	0.340	25.42	0.750	0.279
	UPV	56.18	0.669	0.169	11.98	0.644	0.140	9.78	0.743	0.276	25.98	0.685	0.195
	SWEET	48.07	0.689	0.188	11.68	0.666	0.192	10.24	0.719	0.284	23.33	0.691	0.221
	MorphMark	56.56	0.608	0.103	11.30	0.586	0.100	10.61	0.627	0.120	26.16	0.607	0.108
	KGW+D	53.98	**0.973**	**0.861**	**11.98**	**0.903**	**0.552**	9.78	**0.948**	**0.744**	25.25	**0.941**	**0.719**
	Unigram+D	55.34	**0.919**	**0.626**	**10.99**	**0.863**	**0.520**	10.08	**0.905**	**0.648**	**25.47**	**0.895**	**0.598**
	UPV+D	53.30	**0.871**	**0.550**	10.54	**0.780**	**0.308**	**10.01**	**0.870**	**0.572**	24.62	**0.840**	**0.477**

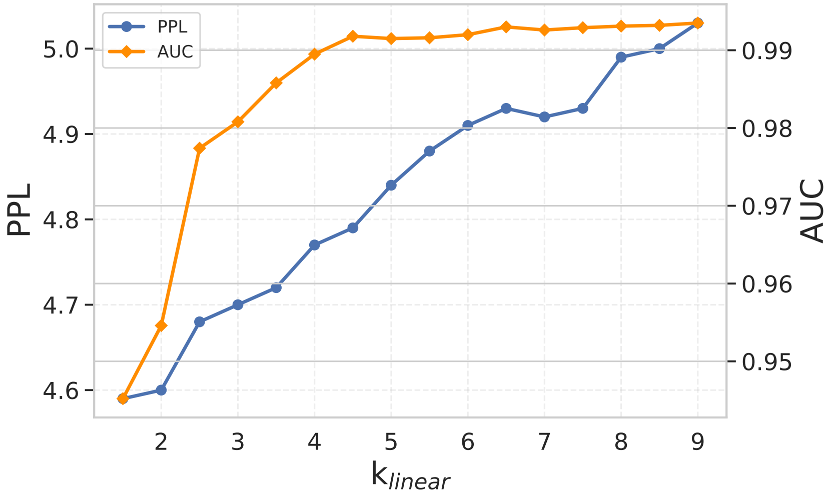

Figure 6: Increasing k_{linear} parameter for MorphMark.